Mathematisches Forschungsinstitut Oberwolfach

Inverse Problems for Partial Differential Equations

Organised by
Martin Hanke-Bourgeois (Mainz)
Andreas Kirsch (Karlsruhe)
William Rundell (Austin)
Matti Lassas (Helsinki)

February 19th – February 25th, 2012

ABSTRACT. This workshop brought together mathematicians engaged in different aspects of inverse problems for partial differential equations. Classical topics such as the inverse problems of impedance tomography and scattering theory as well as new developments such as interior transmission eigenvalues were discussed.

Introduction by the Organisers

This workshop *Inverse Problems for Partial Differential Equations*, organized by Martin Hanke-Bourgeois (Mainz), Andreas Kirsch (Karlsruhe), William Rundell (College Station), and Matti Lassas (Helsinki) was held February 19th to February 25th, 2012. The participants consisted of 23 mathematicians, a nice mixture of researchers with various backgrounds. The participants were the usual international blend and a stimulating mixture of well-established mathematicians and junior scientists. For many in the group this was their first visit to Oberwolfach and, in some cases, their first time to meet each other.

Since the workshop was only a "half workshop" the organizers decided to concentrate on mainly analytical methods where questions of uniqueness and (if appropriate) existence were at the forefront. Although reconstructive methods were not in the center of our focus – also because there will be an Oberwolfach workshop with this particular emphasis later this year – most of the talks did show some illustrative reconstructions. With the smaller number of participants it was possible to have a relaxed schedule and yet allow the most of them to give a talk.

In 18 talks a wide range of aspects was covered in the study of inverse problems for partial differential equations, in particular for the wave equations in the time and frequency domain with their stationary and quasi-stationary approximations, equations from elasticity, and Maxwell's equations.

Three of the submitted talks were chosen on the spot to be highlighted as "expository presentations", which meant that the authors were given up to 90 minutes to present their paper within a broader context and a more detailed introduction to that area. The chosen topics included the celebrated cloaking problem, the various possibilities to use coupled physics imaging techniques, and the inverse helioseismology problem. All participants appreciated this kind of format as a wonderful opportunity to learn more about fascinating applications that have not yet been in the focus of their own specialized research.

All other talks were scheduled for a maximum of 50 minutes to allow for comments and discussions (and frequently the additional post-talk questions and comments took us up to the next speaker). Almost all participants attended all the lectures. A reason for the high attendance was the excellent overall quality of the talks; it is clear that all of the speakers had taken great care over the preparation and there was considerable confidence that talks were modified as the conference progressed in order to present a fresh set of ideas to the audience.

As usual, the service provided by the staff was exemplary. This plays an enormous part in the "Oberwolfach experience" and allows the participants to concentrate on the research projects only.

Workshop: Inverse Problems for Partial Differential Equations

Table of Contents

Abstracts

Electromagnetic Cloaking by Mapping of all Frequencies
Michael Vogelius

The problem: "how may one create a subset in space such that arbitrary objects placed inside that subset are rendered invisible (cloaked) to electromagnetic probing" has recently received quite a bit of attention in the mathematical as well as the applied physics /engineering literature. In this talk I will present some results about a popular scheme of approximate cloaking (approximate cloaking by mapping). In particular I will provide very precise estimates for the degree of cloaking in the context of the Helmholtz equation (at all frequencies) and the scalar wave equation. These estimates are in terms of the degree of anisotropy and the singularity of the "meta materials" used to produce the cloak. In the "extreme limits" they assert that the cloak becomes perfect.

Sampling Methods for Inverse Scattering Problems in the Time Domain
Armin Lechleiter
(joint work with Qiang Chen, Houssem Haddar, Simon Marmorat, Peter Monk)

Inverse scattering problems for waves in the frequency domain enjoy continuous interest in the applied mathematics community since more than 30 years (the monograph [7] is a standard reference). In several applications one is however able to measure wave fields in the time domain. Of course, such measurements can in principle be transformed into multi-frequency data, and one might then choose a suitable frequency for inversion using a frequency-domain algorithm. However, this possibly implies that one looses a significant amount of information contained in the time domain data, and the choice of the optimal frequency is far from trivial. To this end, several recent works consider inversion algorithms that work with multi-frequency data [10, 11, 15], or directly on the time domain data [3, 1, 6, 16]. Some of the underlying ideas come from methods in the frequency domain, whereas others are based on time reversibility [8].

In this talk, we consider two sampling methods for time domain inverse scattering, the linear sampling method [5] and the factorization method [14]. It is worth to note that both methods require measurements for all times, in contrast to some of the above-mentioned techniques. The trade-off is that algorithms working with finite time data cannot yield more information than, roughly speaking, slightly more than the convex hull of the scatterer. (This is essentially due to the finite speed of propagation.) For numerics this means that both methods considered here require to measure scattered fields until most of the wave energy has passed the receivers.

The first version of the linear sampling method in the time domain allows to find the geometry of a (possibly disconnected) scatterer with connect complement from

measurements of causal scattered waves on some measurement surface, see [6]. As in the frequency version of the method, the criterion to decide whether a point is inside or outside the scatterer relies on the approximate solution of a linear integral equation (in time and space) for many right-hand sides. These right-hand sides are time domain point sources at the sampling points. The analysis of the algorithm is based on retarded potentials in exponentially weighted spaces that arise naturally via Laplace transforms. Recent results in [12] extend the method to obstacles with mixed boundary conditions and incident waves that are caused by smooth pulses.

Despite the linear sampling method is a numerically attractive tool for domain reconstruction, its theoretical justification remains limited and does for instance not allow to give a rigorous characterization of the scatterer's shape. In the frequency domain it is well known that the factorization method provides a theoretically sound algorithm for shape reconstruction. Recently, in [13], we showed that the same phenomenon arises in the time domain when one considers far-field measurements. In this case, the time domain far-field operator F possesses a factorization where the outer operators are adjoint to each other. Unfortunately, the middle operator (the inverse to the retarded single-layer operator) is not positive, which implies that the standard theory of the factorization method cannot directly be applied. However, it turns out that the time derivative of the middle operator is positive (this goes back to [2]), and that the time derivative commutes with the outer (Herglotz-like) convolution operator. Thus, the right framework for the method relies on the time derivative $\partial_t F$ of the far-field operator. The question of suitable function spaces for this factorization is relatively involved, since the above mentioned exponentially weighted spaces are not sufficient. We choose polynomially weighted spaces that allow to use Fourier transformation arguments in time (in the sense of $\mathcal{S}'$). The theoretical statement of the method is that the time domain far-field of a point source with source point inside the scatterer belongs to the range of a "square root" of $\partial_t F$. For points outside the closure of the scatterer such far-fields do not belong to the range of this square root. The proof does not allow a statement concerning boundary points, which is related to the fact that the middle operator is positive, but not coercive, compare [9].

References

[1] K. Bingham, Y. Kurylev, M. Lassas and S. Siltanen, *Iterative time-reversal control for inverse problems*, Inverse Probl. Imag. **2** (2008), 63–81.

[2] A. Bamberger and T. Ha Duong, *Formulation variationnelle espace-temps pour le calcul par potentiel retardé dune onde acoustique*, Math. Meth. in Appl. Sci. **8** (1986), 405–435.

[3] L. Borcea, G. Papanicolaou and C. Tsogka, *Adaptive interferometric imaging in clutter and optimal illumination*, Inverse Problems **22** (2006), 1405–1436.

[4] C. Burkard and R. Potthast, *A time-domain probe method for three-dimensional rough surface reconstructions*, Inverse Probl. Imaging **3** (2009), 259–274.

[5] F. Cakoni and D. Colton, *Qualitative methods in inverse scattering theory. An introduction.* Springer, Berlin, 2006.

[6] Q. Chen, H. Haddar, A. Lechleiter and P. Monk, *A sampling method for inverse scattering in the time domain*, Inverse Probl. **26** (2010), 085001.

[7] D. Colton and R. Kress, *Inverse Acoustic and Electromagnetic Scattering Theory*. 2nd edition, Springer, Berlin, 1998.

[8] M. Fink, *Time reversal of ultrasonic fields: basic principles*, IEEE Trans. Ultrason., Ferroelectric and Frequency Control **39** (1992), 555–566.

[9] F. Frühauf, B. Gebauer and O. Scherzer, *Detecting interfaces in a parabolic-elliptic problem from surface measurements*, SIAM J. Numer. Anal. **45** (2007), 810-836.

[10] R. Griesmaier, *Multi-frequency orthogonality sampling for inverse obstacle scattering problems*, Inverse Probl. **27** (2011), 085005.

[11] B. Guzina, F. Cakoni and C. Bellis, *On the multi-frequency obstacle reconstruction via the linear sampling method*, Inverse Probl. **26** (2010), 125005.

[12] H. Haddar, A. Lechleiter, and S. Marmorat, *Une méthode d'échantillonnage linéaire dans le domaine temporel: le cas des obstacles de type Robin-Fourier*, Rapport de recherche INRIA No. 7835, 2011, online at `http://hal.inria.fr/hal-00651301`.

[13] H. Haddar and A. Lechleiter, *A factorization method for a far-field inverse scattering problem in the time domain*, accepted for Comm. Part. Diff. Eq., 2012.

[14] A. Kirsch and N. Grinberg, *The factorization method for inverse problems*, Oxford University Press, Oxford, 2008.

[15] D. R. Luke and R. Potthast, *The point source method for inverse scattering in the time domain*, Math. Meth. Appl. Sci. **29** (2006), 1501–1521.

[16] L. Oksanen, *Solving an inverse problem for the wave equation by using a minimization algorithm and time-reversed measurements*, Inverse Probl. Imag. **3** (2011), 731–744.

Multilevel Bayesian reconstruction in impedance tomography

MARTIN SIMON

(joint work with Martin Hanke and Petteri Piiroinen)

We consider the conductivity equation

$$\nabla \cdot (\kappa \nabla u) = 0$$

posed on a bounded, simply connected domain $D \subset \mathbb{R}^d$, $d = 2, 3$, with smooth boundary ∂D. The (possibly anisotropic) conductivity is modeled by a measurable, symmetric matrix-valued function $\kappa : D \to \mathbb{R}^{d \times d}$ such that for all indices $i, j \leq d$, $i \neq j$, $\text{supp}(\kappa_{ij})$ and $\text{supp}(\kappa_{ii} - 1)$ are compact subsets of D and κ is uniformly elliptic, that is we have

$$C^{-1} ||\xi||^2 \leq \xi \cdot \kappa(x)\xi \leq C||\xi||^2, \quad \text{for } \xi \in \mathbb{R}^d, \text{ a.e. } x \in D$$

and some constant $C > 0$. We study discrete voltage-to-current measurements performed using N electrodes E_l, $l = 1, ..., N$ on the boundary ∂D based on the complete electrode model. In this model the electric potential u satisfies the Robin boundary condition

$$\partial_\nu u + fu|_{\partial D} = g,$$

where ν denotes the outer unit normal on ∂D and $f, g : \partial D \to \mathbb{R}$ are given by

$$f(x) := z^{-1} \sum_{l=1}^{N} \chi_{E_l}(x), \quad g(x) := z^{-1} \sum_{l=1}^{N} U_l \chi_{E_l}(x).$$

Here, $z \in \mathbb{R}^+$ is the so-called *contact impedance*, χ_{E_l} is the indicator function of the l-th electrode and $U = (U_1, ..., U_N)^T$ denotes the prescribed voltage pattern.

The voltage-to-current map is given by the linear self-adjoint operator mapping voltage patterns to current vectors $J = (J_1, ..., J_N)^T$,

$$J_l = \int_{E_l} \partial_\nu u \mathrm{d}\sigma(x), \quad l = 1, ..., N,$$

where σ is the Lebesgue surface measure on ∂D.

The inverse problem of impedance tomography is to recover κ from the voltage-to-current map. A numerical solution to this problem may be computed using the framework of Bayesian inversion, see e.g. [8]. The basic idea is to consider a discrete measurement model of the form

$$y = F(\theta) + e,$$

where $\theta \in \mathbb{R}^M$ denotes the vector of unknown parameters, i.e. the parameterized conductivity and y the measured data, that is the vector of electrode currents $F(\theta)$ computed by the forward solver F plus an additive measurement error e. By Bayes' theorem, the posterior probability density of the unknown θ satisfies

$$\pi(\theta|y) \propto \pi(y|\theta)\pi(\theta).$$

In this talk we are interested in approximating the conditional mean estimate

$$\int_{\mathbb{R}^M} \theta \pi(\theta|y) \mathrm{d}\theta,$$

which is usually done using Markov chain Monte Carlo. A major drawback, however, is the high computational time due to numerous forward solves for exploration of the posterior density. In practice the computational cost is sometimes reduced by using a first-order Taylor series approximation to yield a linearization of the problem around a feasible solution guess. However, due to the ill-posedness of the inverse problem the error in the forward model F should be negligible compared to the measurement error but there is no information available on the probability distribution of the perturbation resulting from linearization.

We propose an alternative forward model based on a Feynman-Kac-type formula for the voltage-to-current map which yields a hierarchy of approximations, each computable in a parallel manner and endowed with a probabilistic error estimate.

It is well-known that symmetric Markov processes can be associated with self-adjoint operators via Dirichlet form theory, see [4]. If κ has components that are sufficiently smooth, say in $C^{1,1}(\overline{D})$, then it is a classical result that there is a continuous strong Markov process $(\Omega, \mathcal{F}, \mathcal{F}_t, X, P^x, x \in \overline{D})$ associated with the operator $\nabla \cdot (\kappa \nabla \cdot)$ defined on an appropriate domain, which is called the *reflecting diffusion process* on $\overline{D}$. X has the following Skorohod decomposition:

$$(1) \qquad X_t = x + \int_0^t a(X_s)\mathrm{d}s + \int_0^t B(X_s)\mathrm{d}W_s - \int_0^t \nu(X_s)\mathrm{d}L_s$$

where $a = (a_1, ..., a_d)^T$, $a_i = \sum_{j=1}^d \partial_j \kappa_{ij}$, $i = 1, ..., d$, $B : \overline{D} \to \mathbb{R}^{d \times d}$ denotes the diffusion matrix satisfying $\kappa = \frac{1}{2}BB^T$, W is a standard d-dimensional Brownian motion and L is a positive continuous additive functional of X corresponding to the Lebesgue surface measure on ∂D via the Revuz correspondence. For general

κ with merely measurable components, an associated continuous strong Markov process, which we denote by $(\Omega, \mathcal{F}, \mathcal{F}_t, X, P^x, x \in \overline{D})$ as well, can be constructed analytically by proving a strong Feller property of the resolvent, see [5].

In [7] a generalized Feynman-Kac-type representation formula for the electrode currents is established, namely if $(u, J) \in H^1(D) \oplus \mathbb{R}^N$ is the solution to the forward problem for voltage pattern $U \in \mathbb{R}^N$, then

$$(2) \qquad J_l = \left\langle \mathbb{E}^x \left[z^{-1} \left(U_l - \int_0^\tau g(X_t) \mathrm{d}L_t \right) \right] \right\rangle_x,$$

where

$$\tau = \inf \left\{ t : \int_0^t f(X_s) \mathrm{d}L_s > Z \right\}, \quad Z \sim \mathrm{Exp}(1)$$

and Z is independent of X. The notation $\langle \cdot \rangle_x$ in (2) denotes the expectation with respect to the uniform initial distribution $x \sim \mathcal{U}(E_l)$.

As an application of this formula we study the computation of the conditional mean estimate. For this purpose we introduce a probabilistic forward solver that combines time discretization of the stochastic differential equation (1) with the half-space approximation developed in [6] and simulation of L exploiting a result from [9]. For generating pseudorandom numbers we use the NAG implementation of L'Ecuyer's MRG32k3a generator, see [2]. The resulting forward solver turns out to be highly efficient on parallel GPUs, as the runtime scales linearly with the number of kernels.

Finally we discuss a multilevel hybrid probabilistic deterministic Metropolis Hastings algorithm, that takes advantage of the probabilistic forward solver. The basic idea is to use a hierarchy of probabilistic low-resolution forward models to approximate draws from a posterior distribution that is based on a high-resolution forward model with discretization error negligible compared to the measurement error. For the low-resolution forward models, computational efficiency is achieved through parallel simulation of merely a small number of sample paths of X. The acceptance probability is estimated using statistics from the probabilistic forward solver and an approximate confidence interval for the true acceptance probability, cf. [1]. That is, a proposal is only accepted if this can be done with a certain confidence, otherwise either the level is increased or, if the confidence on the initial level is below some given bound, a deterministic forward solver based on finite elements is employed right away. Numerical experiments for $d = 3$ show both, better reconstructions compared to sampling with a linearized forward map and a significant speed up compared to the two-level algorithm from [3] using a high-resolution finite element based forward solver.

We should emphasize, however, that our probabilistic forward solver is only applicable for κ with components in $C^{1,1}(\overline{D})$. While the representation (2) remains true, the process X has no need to be a semimartingale in general. The question how to simulate such processes for the special case of piecewise constant κ is subject of ongoing research.

REFERENCES

[1] G. Bal, I. Langmore and Y. Marzouk, *Bayesian inverse problems with Monte Carlo forward models*, Preprint, 2011.
[2] P. L'Ecuyer *Good parameter sets for combined multiple recursive random number generators*, Operations Research, **47** (1999), 159–164.
[3] Y. Efendiev, T. Hou and W. Luo, *Preconditioning Markov chain Monte Carlo simulations using coarse-scale models*, SIAM J. Sci. Comput., **28** (2006), 776–803.
[4] M. Fukushima, Y. Ōshima and M. Takeda, Dirichlet forms and symmetric Markov processes, de Gruyter, Berlin, 1994.
[5] M. Fukushima and M. Tomisaki, *Construction and decomposition of reflecting diffusions on Lipschitz domains with Hölder cusps*, Probab. Theory Related Fields **106** (1996), 521–557.
[6] E. Gobet, *Efficient schemes for the weak approximation of reflected diffusions*, Monte Carlo Methods Appl. **7** (2001), 193–202.
[7] P. Piiroinen and M. Simon, *A Feynman-Kac-type formula for impedance tomography*, in preparation.
[8] J. P. Kaipio, V. Kolehmainen, E. Somersalo and M. Vauhkonen, *Statistical inversion and Monte Carlo sampling methods in electrical impedance tomography*, Inverse Problems **16** (2000), 1487–1522.
[9] D. Lépingle, *Euler scheme for reflected stochastic differential equations*, Math. Comput. Simulation, **38** (1995), 119–126.

Fractional Brownian motion and asymptotic Bayesian estimation

PETTERI PIIROINEN

(joint work with Lassi Päivärinta)

We study the problem of estimating the *Hurst parameter* from a finite and discrete sample of single realisation of fractional Brownian motion. This presentation is based on [4].

The fractional Brownian motion Z^H is a one parameter generalization of the standard Brownian motion B introduced in [3]. The generalization corresponds to changing the variance function $\mathbf{V}B_t = |t|$ to the variance function $\mathbf{V}Z_t = |t|^{2H}$ where the Hurst parameter $H \in (0, 1)$. It can be shown that with this choice the fractional Brownian motion exists as a stochastically continuous Gaussian process with stationary increments. These increments are not, however, independent unless $H = \frac{1}{2}$ which corresponds to the Brownian motion case. This makes the analysis of these processes more involved.

The inverse problem we have in mind is the usual parameter estimation problem. We sample a given signal $X^{\widehat{H}}$ at equidistant time instances $t_j = j/n$ for every $j = 0, 1, \ldots, n$. From this data we form the increments $Y_j^{\widehat{H}} := X^{\widehat{H}}(t_j) - X^{\widehat{H}}(t_{j-1})$. The reason for using the increments is motivated by the stationarity.

We formulate the parameter estimation problem as the Bayesian estimation problem:

> *Determine the conditional probability distribution of H given the sample $(Y_1^{\widehat{H}}, \ldots, Y_n^{\widehat{H}})$. From the conditional probability distribution construct estimators for the true parameter $\widehat{H}$.*

We solve this using the standard Bayesian methods with the assumption that the prior is noninformative. This leads to the solution of form

$$\mathbf{P}(H \in U \,|\, \xi_{\widehat{H},n}) = C_n(\xi_{\widehat{H},n}) \int_U \frac{n^{nu}}{\sqrt{|T_n(f_u)|}} e^{-\frac{1}{2}n^{2(u-\widehat{H})}Q_n(\xi_{\widehat{H},n},u)} \mathrm{d}u$$

where $T_n(f)$ is the $n \times n$ Toeplitz matrix corresponding to the symbol f, the $|\cdot|$ stands for the determinant and where Q_n is the quadratic form

$$Q_n(y,u) = \langle y, T_n(f_u)^{-1}y \rangle.$$

The data $\xi_{\widehat{H},n}$ we use in the posteriori solution is the rescaled increments $\xi_{,n} := n^{\widehat{H}}(Y_1^{\widehat{H}}, \ldots, Y_n^{\widehat{H}})$. The symbol f_u corresponds to the covariance operator of the increments of fractional Brownian motion Z^u sampled at integer points.

This solution leads immediately to a numerical reconstruction method. However, the computational cost of numerically calculating the quadratic form Q_n is both expensive and quite unstable. Moreover, the computation of the Toeplitz determinant is likewise rather expensive and unstable. Therefore, only relatively small values of n can be used in numerical analysis and for small n the reconstruction from a simulated data does not appear to be very consistent with the true parameter value.

The question we wanted to analyse is how these distributions behave asymptotically as the number n of samples tends to infinity. The first time the problem was studied by d'Ambrogi–Ola [1]. In [1] the inverse matrix $T_n(f_u)^{-1}$ was replaced by a well-motivated approximation. This led to an approximate solution of the inverse problem and in [1] the corresponding approximate maximum aposteriori (MAP) estimate was shown to converge to $\widehat{H}$ provided that $\widehat{H} > \frac{1}{2}$.

In this presentation we tackle the original problem without using approximations. We show as a corollary that the posteriori distribution converge weakly to point mass on top of $\widehat{H}$ almost surely. This follows from the characterization result for the asymptotic conditional distribution. More precisely, we show in [4] that with probability one the conditional distribution of $\widetilde{H}_n$ is asymptotically standard normal with mean α_n where the random variable $\widetilde{H}_n$ is a rescaled version of the random variable H. As a part of this result we deduce that the asymptotic variance of H around the mean α_n is of order $n^{-1}(\log n)^{-2}$. Furthermore, we show that the means α_n converge to $\widehat{H}$ as $n \to \infty$ with a rate of order $(\log n)^{-2}$.

From this asymptotic normality we can read that the usual estimators like conditional mean and the MAP estimates are biased for large n but they are asymptotically unbiased and asymptotically exact. The rates of convergences of the means and the variances in particular imply that for large n the reconstructions would be very peak like but the peak is likely to close to the true value but at incorrect place.

In the proof of the asymptotic parameter estimation result we use the asymptotics for Toeplitz determinants with one Fisher–Hartwig singularity [2]. In order to handle the randomness coming from the random quadratic form, we prove the *Strong Law of Large Numbers (SLLN)* for the quadratic form Q_n appearing in the

posteriori distribution. This SLLN is the most involved part of [4] and proving it requires different techniques from probability theory, some ideas from the theory of Toeplitz operators and asymptotics for the inverse Toeplitz matrices [5, 6].

REFERENCES

[1] B. d'Ambrogi–Ola, *Inverse Problem for Fractional Brownian Motion with Discrete Data*, Ph.D. thesis, University of Helsinki, (2009).
[2] T. Ehrhardt, B. Silbermann, *Toeplitz Determinants with one Fisher–Hartwig Singularity*, J. Funct. Anal. **148** (1997), 229–256.
[3] B. B. Mandelbrot, J. W. Van Ness, *Fractional Brownian motions, fractional noises and applications*, SIAM Rev. **10** (1968), 422–437.
[4] L. Päivärinta, P. Piiroinen, *Fractional Brownian motion and asymptotic Bayesian estimation*, almost submitted.
[5] P. Rambour, A. Seghier, *Théorèmes de trace de type Szegő dans le cas singulier*, Bull. Sci. Math. **129** (2005), 149-174.
[6] P. Rambour, A. Seghier, *Inverse asymptotique des matrices de Toeplitz de symbole $(1-\cos\theta)^\alpha f_1$, $1/2 < \alpha \leq 1/2$, et noyaux intégraux*, Bull. Sci. Math. **134** (2010), 155-188.

Electrical impedance tomography with two electrodes

NUUTTI HYVÖNEN

(joint work with Otto Seiskari)

Electrical impedance tomography (EIT) is an imaging technique for recovering information about the conductivity distribution inside a physical body from boundary measurements of current and voltage. It has applications, e.g., in medical imaging, process tomography and nondestructive testing of materials; see the review articles [2, 10] and the references therein. In this work we consider EIT in the special case that the boundary measurements are performed with only two electrodes, one of which can be moved along the object boundary.

The conductivity distribution inside the two-dimensional, smooth, bounded and simply connected object of interest $D \subset \mathbb{R}^2$ is assumed to be of the form

$$(1) \qquad \sigma(x) = \begin{cases} \kappa_j & \text{if } x \in \Omega_j, \quad j = 1, \ldots, m, \\ 1 & \text{otherwise,} \end{cases}$$

where $\kappa_1, \ldots, \kappa_m > 0$ are constant conductivity levels and the inclusions $\Omega_1, \ldots, \Omega_m$ are bounded Lipschitz domains with connected complements, such that

$$\overline{\Omega}_i \cap \overline{\Omega}_j = \emptyset \quad \text{for all } i \neq j \qquad \text{and} \qquad \Omega := \bigcup_{j=1}^m \Omega_j \subset\subset D.$$

We consider the elliptic boundary value problem

$$(2) \qquad \nabla \cdot (\sigma \nabla u) = 0 \quad \text{in } D, \qquad \frac{\partial u}{\partial \nu} = f \quad \text{on } \partial D,$$

where ν is the exterior unit normal field of ∂D. For a current density f in

$$(3) \qquad H^s_\diamond(\partial D) = \{g \in H^s(\partial D) \,|\, \langle g, 1\rangle_{\partial D} = 0\}, \quad s \in \mathbb{R},$$

the problem (2) has a unique solution u_σ in $H^{\min\{1,s+3/2\}}(D)/\mathbb{C}$; cf., e.g., [7]. Moreover, the Neumann-to-Dirichlet map

$$\Lambda : f \mapsto u_\sigma|_{\partial D}, \qquad H^s_\diamond(\partial D) \to H^{s+1}(\partial D)/\mathbb{C},$$

is well defined and bounded for every $s \in \mathbb{R}$ [7], and the same is also true for the reference map

$$\Lambda_{\mathbf{1}} : f \mapsto u_{\mathbf{1}}|_{\partial D}, \qquad H^s_\diamond(\partial D) \to H^{s+1}(\partial D)/\mathbb{C},$$

where $u_{\mathbf{1}} \in H^{s+3/2}(D)/\mathbb{C}$ is the unique solution of (3) when $\sigma \equiv 1$. Because σ of (1) is assumed to be identically 1 in some interior neighborhood of ∂D, it follows that the difference Neumann-to-Dirichlet map

(4) $$\Lambda - \Lambda_0 : H^{-s}_\diamond(\partial D) \to H^s(\partial D)/\mathbb{C}$$

is bounded for any $s \in \mathbb{R}$ [7].

Let us consider a specific localized current pattern, namely $f = \delta_z - \delta_{z_0} \in H^{-1/2-\epsilon}_\diamond(\partial D)$, $\epsilon > 0$, with $z, z_0 \in \partial D$ and δ_y denoting the delta distribution located at y on ∂D. Due to the boundedness of the boundary operator (4), the quantity

$$\varsigma_\sigma(z) = \langle (\delta_z - \delta_{z_0}), (\Lambda - \Lambda_{\mathbf{1}})(\delta_z - \delta_{z_0}) \rangle_{\partial D}$$

is well defined. The function $\varsigma_\sigma : \partial D \to \mathbb{R}$ is called the sweep data of EIT [4], and it can be approximated in practice as follows [6]: Unit current is maintained between two small electrodes at z_0 and z while the latter is moved along ∂D in a sweeping motion. The corresponding potential difference between the electrodes is recorded as a function of z, and the actual sweep data is finally obtained by subtracting the corresponding measurement in the case that $\sigma \equiv 1$. According to [4], ς is the trace of a holomorphic function defined in $D \setminus \overline{\Omega}$.

In [8] a holomorphic asymptotic expansion is derived for the (extended) sweep data with respect to the size of the inclusions in (1). This is a generalization to a less regular framework of an analogous result in [5]. The leading order term in the asymptotic expansion of the sweep data turns out to be a complex rational function that has poles only inside the inclusions. This observation makes it possible to adopt from [5] an idea for locating several small inclusions: certain Laurent–Padé approximants [1] are computed for the sweep data and the corresponding poles are considered as estimates for the positions of the inhomogeneities. The paper [8] also introduces a novel method for estimating the strengths of the inclusions by manipulating the residues of the Laurent–Padé approximants. The algorithm generalizes straightforwardly to any bounded, smooth and simply connected planar domain with the help of conformal mappings.

The functionality of the reconstruction method is demonstrated by numerical experiments based on simulated and real-life data. In addition to testing the algorithm with two-dimensional domains and point electrodes, three-dimensional cylindrical objects and electrodes of realistic size are considered in the framework of the *complete electrode model* [3, 9].

REFERENCES

[1] G. Baker and P. Graves-Morris, *Padé approximants*, Cambridge University Press, 1996.
[2] L. Borcea, *Electrical impedance tomography*, Inverse Problems **18** (2002), R99–R136.
[3] K-S. Cheng, D. Isaacson, J. C. Newell and D. G. Gisser, *Electrode models for electric current computed tomography*, IEEE Trans. Biomed. Eng. **36** (1989), 918–294.
[4] H. Hakula, N. Hyvönen and L. Harhanen, *Sweep data of electrical impedance tomography*, Inverse Problems, **27** (2011), 115006.
[5] M. Hanke, *Locating several small inclusions in impedance tomography from backscatter data*, SIAM J. Numer. Anal. **49** (2011), 1991–2016.
[6] M. Hanke, B. Harrach and N. Hyvönen, *Justification of point electrode models in electrical impedance tomography*, Math. Models Methods Appl. Sci. **21** (2011), 1395–1413.
[7] M. Hanke, N. Hyvönen and S. Reusswig, *Convex backscattering support in electric impedance tomography*, Numer. Math. **117** (2011), 373–396.
[8] N. Hyvönen and O Seiskari, *Detection of multiple inclusions from sweep data of electrical impedance tomography*, submitted.
[9] E. Somersalo, M. Cheney and D. Isaacson, *Existence and uniqueness for electrode models for electric current computed tomography*, SIAM J. Appl. Math. **52** (1992), 1023–1040.
[10] G. Uhlmann, *Electrical impedance tomography and Calderón's problem*, Inverse Problems **25** (2009), 123011.

Photoacoustic and Coupled Physics Imaging

OTMAR SCHERZER

(joint work with Peter Elbau, Andreas Kirsch, Rainer Schulze)

There exist various reconstruction formulas and back-projection algorithms for *photoacoustic imaging* (see the survey [4] and the references therein). Also different measurement devices for the ultrasound pressure have been suggested. Most common are small detectors based on materials, which exhibit a strong piezoelectric effect and can be immersed safely in water (i.e. polymers such as PVDF). In analytical reconstruction formulas, they are considered point detectors. Other experimental setups have been realized with line and area detectors, which collect averaged pressure (see [9] for a survey).

Here, we consider the problem of photoacoustic *sectional imaging*. Opposed to standard photoacoustic imaging, where the detectors record sets of two-dimensional projection images from which the three-dimensional imaging data can be reconstructed, *single slice imaging* reconstructs a set of two-dimensional slices, each by a single scan procedure. The advantages of the latter approach are a considerable increase in measurement speed and the possibility to do selective plane imaging. In general, this can only be obtained by the cost of decreased out-of-plane resolution. The difference in this model to previously studied models is that the wave propagation is considered fully three-dimensional, the initialization *and* measurements are fully two-dimensional due to the selective plane illumination and detection. Therefore, such setups require novel reconstruction formulas, which have been explained in this talk. After the introduction of the *universal* back-projection algorithm introduced in [11] this goal seems superfluous. However, it has been shown recently by Natterer [6] that *universal* back-projection is only exact for

special sampling geometries. Here, for sliced imaging and certain sampling setups, we can indeed find mathematically exact universal reconstruction algorithms for arbitrary strictly convex sampling domains Ω.

We model the sectional photoacoustic imaging by assuming that the *initial pressure distribution* $f : \mathbb{R}^3 \to \mathbb{R}$ is perfectly focused in the illumination plane $\{x \in \mathbb{R}^3 \mid x_3 = 0\}$:

$$(1) \qquad f(\xi, z) = \hat{f}(\xi)\delta(z), \quad \xi \in \mathbb{R}^2, \ z \in \mathbb{R},$$

for some smooth function $\hat{f} : \mathbb{R}^2 \to \mathbb{R}$. The resulting pressure wave $p : \mathbb{R}^3 \times [0, \infty) \to \mathbb{R}$, we assume to be the solution of the linear three-dimensional wave equation

$$(2) \qquad \boxed{\begin{aligned} \partial_{tt}p(\xi, z; t) &= \Delta_{\xi,z}p(\xi, z; t), \\ \partial_t p(\xi, z; 0) &= 0, \\ p(\xi, z; 0) &= f(\xi, z) = \hat{f}(\xi)\delta(z) \end{aligned}}$$

for all $\xi \in \mathbb{R}^2$, $z \in \mathbb{R}$, and $t > 0$. Here,

$$\Delta_{\xi,z} = \partial_{\xi_1 \xi_1} + \partial_{\xi_2 \xi_2} + \partial_{zz}$$

denotes the three-dimensional Laplacian in Euclidean coordinates.

The goal of sectional imaging is to recover the function $\hat{f}$, describing the initial pressure distribution, from certain measurements of the pressure wave p. The position of the detectors performing these measurements shall be given by the boundary $\partial\Omega$ of a convex domain $\Omega \subset \mathbb{R}^2$ in the illumination plane, where we additionally assume that $\hat{f}$ has compact support in Ω.

Sectional imaging has become experimentally tractable [5, 10, 2, 3]. The following mathematical work also shows that it can be used to determine other imaging modalities, such as the wave speed variations by photoacoustic measurements, by using backprojection formulas. Opposed to *sectional 3D photoacoustic imaging*, where stacks of complementary two-dimensional projection images are produced, the proposed approach for simultaneous imaging consists in performing overlapping sliced imaging by rotation and translation of the specimen. This also generates enough data for reconstructing the two independent parameter functions, speed of sound and absorption density. Exact reconstruction formulas for the wave speed function in ultrasound reflectivity tomography are based on the *Born approximation* to the wave equation, which is valid for moderately varying speed of sound. Reconstruction formulas for ultrasound reflectivity tomography have already been derived by Norton & Linzer [7, 8] and are also based on inversion formulas for the spherical mean operator. The possibility of exact inversion in both fields supports to derive exact inversion formulas for both parameters, which is outlined in this talk.

The reconstruction formulas for simultaneous imaging utilize techniques from reflectivity imaging and photoacoustic imaging. In the current state of research we can provide exact reconstruction formulas, but use way too much data. The

practical criticism with our approach is that, due to physical constraints, sectional imaging is applicable to elongated objects. Current sectional photoacoustic imaging experiments, which, however, do not perform wave speed estimation, sample along a cylinder and do not require to steer the sections in all angular directions. In this case, however, currently, there do not exist analytical back-projection formulas for both parameters, the absorption density and wave speed function. Numerical reconstruction methods based on regularization, similar as proposed in [13, 12], have to be implemented. For practical applications we are thinking of an intermediate model, where a cylinder containing the specimen is slightly tilted. This experimental suggestion does not contradict with the assumptions of sectional imaging. In fact these experiments could also be used in combination with a photoacoustic spiral tomograph approach (see [1], which however did not elaborate on simultaneous identification of the wave speed and absorption density, but only on the later). This paper serves as a case study for deriving more complex reconstruction formulas for advanced sampling geometries. We intend to report on numerical studies in a follow up paper. Finally we mention that P. Elbau (RICAM, Linz, Austria) has recently discovered that one measurement in time for each section is sufficient to reconstruct both parameters - in his approach, although using significantly less data, the complex steering of the experiment is still required, only the time measurements can be performed shorter.

References

[1] T. Fidler. Thermoacoustic tomography. Master thesis, University of Innsbruck, Austria, Innsbruck, March 2006.

[2] Sibylle Gratt, Klaus Passler, Robert Nuster, and Guenther Paltauf. Photoacoustic imaging with a large, cylindrical detector. In *Digital Holography and Three-Dimensional Imaging*, page JMA51. Optical Society of America, 2010.

[3] Sibylle Gratt, Klaus Passler, Robert Nuster, and Guenther Paltauf. Photoacoustic section imaging with an integrating cylindrical detector. In Henricus J. C. M. Sterenborg and I. Alex Vitkin, editors, *Novel Biophotonic Techniques and Applications*, volume 8090, page 80900K. SPIE, 2011.

[4] Peter Kuchment and Leonid Kunyansky. Mathematics of thermoacoustic tomography. *European J. Appl. Math.*, 19(2):191–224, 2008.

[5] Rui Ma, Adrian Taruttis, Vasilis Ntziachristos, and Daniel Razansky. Multispectral optoacoustic tomography (msot) scanner for whole-body small animal imaging. *Opt. Express*, 17(24):21414–21426, Nov 2009.

[6] Frank Natterer. Photo-acoustic inversion in convex domains. *preprint*, 2011.

[7] Stephen J. Norton. Reconstruction of a two-dimensional reflecting medium over a circular domain: exact solution. *J. Acoust. Soc. Amer.*, 67(4):1266–1273, 1980.

[8] Stephen J. Norton and Melvin Linzer. Ultrasonic reflectivity imaging in three dimensions: Exact inverse scattering solutions for plane, cylindrical, and spherical apertures. *Biomedical Engineering, IEEE Transactions on*, BME-28(2):202 –220, feb. 1981.

[9] Günther Paltauf, Robert Nuster, Markus Haltmeier, and Peter Burgholzer. Photoacoustic tomography with integrating area and line detectors. In *Photoacoustic Imaging and Spectroscopy*, pages 251–263. CRC Press, 2009

[10] D. Razansky, M. Distel, C. Vinegoni, R. Ma, N. Perrimon, R.W. Köster, and V. Ntziachristos. Multispectral opto-acoustic tomography of deep-seated fluorescent proteins in vivo. *Nature Photonics*, 3(7):412–417, 2009.

[11] Minghua Xu and Lihong V. Wang. Universal back-projection algorithm for photoacoustic computed tomography. *Phys. Rev. E*, 71:016706, Jan 2005.

[12] Z. Yuan and H. Jiang. Three-dimensional finite-element-based photoacoustic tomography: Reconstruction algorithm and simulations. *Med. Phys.*, 34:538–546, 2007.

[13] Z. Yuan, Q. Zhang, and H. Jiang. Simultaneous reconstruction of acoustic and optical properties of heterogeneous media by quantitative photoacoustic tomography. *Opt. Express*, 14:6749–6754, 2006.

Inverse scattering problem for an obstacle with impedance boundary

JIJUN LIU

(joint work with Mourad Sini and Haibing Wang)

The inverse scattering problems for acoustic waves or electromagnetic waves are of great importance both in mathematical theory and in engineering areas. For given incident wave and an obstacle, there will be scattered wave outside of the obstacle due to the reflection of obstacle boundary. The inverse scattering problems aim to detect the properties of the obstacle boundary, say, geometric shape and physical parameters on the boundary, from the information about the scattered waves. Mathematically, these problems can be described by corresponding inverse problems for Helmholtz equation or Maxwell equations under some assumptions.

The acoustic wave scattering by an impenetrable cylinder with infinite length in $\mathbb{R}^3$ can be governed by the following 2-dimensional exterior problem for the Helmholtz equation:

$$
(1) \quad
\begin{cases}
\Delta u + k^2 u = 0 & \text{in } \mathbb{R}^2 \setminus \overline{D}, \\
u = 0 & \text{on } \partial D_D, \\
\frac{\partial u}{\partial \nu} + ik\lambda u = 0 & \text{on } \partial D_I, \\
\lim_{r \to \infty} r^{\frac{1}{2}} \left(\frac{\partial u^s}{\partial r} - iku^s \right) = 0,
\end{cases}
$$

where $D \subset \mathbb{R}^2$ with boundary $\partial D = \overline{\partial D_D} \bigcup \overline{\partial D_I}$ is the 2-dimensional cross of the cylinder, $u = u^i + u^s$ is the total wave outside of D corresponding to the incident plane wave $u^i(x) = e^{ikx \cdot d}$ with wave number k and incident direction d. The last condition is the so-called Sommerfeld radiation condition, which guarantees the outgoing wave at infinite place.

It is well-known that the scattered wave has the following asymptotic

$$
(2) \quad u^s(x) = \frac{e^{ik|x|}}{\sqrt{|x|}} \left(u^\infty(\hat{x}) + O(\frac{1}{|x|}) \right), \quad |x| \to \infty
$$

with $\hat{x} = \frac{x}{|x|}$, the unit vector in $\mathbb{R}^2$. The inverse scattering problem aims to identify the obstacle boundary ∂D_D and ∂D_I as well as the boundary impedance $\lambda(x)$ in ∂D_I from the far field data $u^\infty(\hat{x})$.

The first issue to the above inverse scattering problem is the uniqueness, i.e., can $u^\infty(\hat{x})$ determine $(\partial D_D, \partial D_I, \lambda(x))$? This problem has been answered very well in recent years for different configurations such as $\partial D_D = \emptyset$ or $\partial D_I = \emptyset$, see [3, 7, 8]. More precisely, if the far-field data u^∞ are given at all measurement points $\hat{x}$ for

all incident directions d, then the boundary information $(\partial D_D, \partial D_I, \lambda(x))$ can be determined uniquely.

The second problem is how to extract the boundary information from the far-field data, i.e., we need to construct the implementable reconstruction scheme from finite number of measurement data, which are the main topic of our talk.

Roughly speaking, there are two different schemes to reconstruct the obstacle boundary. The first kind of scheme is the approximate method for finite measurement data which uses the optimization technique from which the solution is defined as the minimizer of some cost functional, for example see [5]. The second kind of scheme is the exact method for which the solution can be expressed exactly from some indicator functions, see [1, 2, 6, 12].

Firstly, we introduce how to implement the probe method in the case of $\partial D_D = \emptyset$, which belongs to the so-called "exact method". In the theoretical construction of this scheme [7], the far-field data for the incident plane waves are firstly transformed into the near fields and then these near fields are applied to construct the scattered waves $\Phi^s(\cdot, z)$ corresponding to the point sources. Using $\Phi^s(\cdot, z)$, the Dirichlet to Neumann (DtN) map can be determined from which the indicator for the boundary shape is constructed. Hence the realization of DtN map is a key step in the probe method.

For given Dirichlet data f, the Neumann data $\frac{\partial w}{\partial \nu}\big|_{\partial \Omega} := \Lambda_{\partial D} f$ satisfies

$$(3) \qquad \frac{1}{2}\frac{\partial w(y)}{\partial \nu(y)} - \int_{\partial \Omega} \frac{\partial G(x,y)}{\partial \nu(y)}\frac{\partial w(x)}{\partial \nu(x)}ds(x) = -\frac{\partial}{\partial \nu(y)}\int_{\partial \Omega} f(x)\frac{\partial G(x,y)}{\partial \nu(x)}ds(x)$$

with $G(x, y) := \Phi(x, y) + \Phi^s(x, y), y \in \partial \Omega$. So the key part is to reconstruct the derivatives of $\Phi^s(x, y)$ efficiently.

For this problem we have given a theoretical analysis on the error estimate for the DtN map in terms of the error of far field data, which says that the stability of DtN map is between δ^α and $\left(\ln\frac{1}{\delta}\right)^{-m}$ for any $\alpha \in (0, 1]$ and positive integer m [10]. For reconstruction scheme, we give an efficient realization of the derivative of $\Phi^s(x, y)$ in terms of the reciprocity principle [11]. Once the obstacle shape is determined, the surface impedance can be determined using moment method or boundary integral equation method.

Secondly, we show how to identify the whole system $(\partial D_D, \partial D_I, \lambda(x))$ from far field data corresponding to all incident directions d. By constructing some indicator functions in terms of far field and the approximations to dipole $\Phi(x, y)$ and multipoles $\partial_{x_1}\Phi(x, y), \partial_{x_1 x_2}\Phi(x, y)$ using the Herglotz wave functions, we have proven that $(\partial D_D, \partial D_I, \lambda(x))$ can be determined from far field and we also give its numerical realizations, see [8, 9]. Compared with the probe method, this new scheme constructs indicator functions from the far field directly, without the necessity of transforming far field into near field. Also, based on the high order expansions of the indicators, more subtle information such as the curvature of the obstacle boundary can be extracted. The indicator asymptotic behaviors depend on the boundary curvature and the surface impedance, which provide a potential

application to make the target visible or invisible by introducing suitable surface impedance.

Finally, we introduce our recent work of reconstructing $(\partial D_I, \lambda(x))$ in the case $\partial D_D = \emptyset$ from far field data using the method of fundamental solution (MFS). This method is originally developed for solving direct problems for which the fundamental solution to the PDE can be expressed explicitly. Recently, this method is also applied for solving inverse problems for example, see [4]. This scheme belongs to the approximate method.

For inverse scattering problem, we firstly transform the far-field data into near field on a known cycle $\partial G = \partial B(0, R_0)$ containing the unknown obstacle D. The exact nonlocal DtN condition can be set up on ∂G. Thus the scattered wave satisfies the following problem in a bounded domain:

$$(4) \quad \begin{cases} \Delta u^s + k^2 u^s = 0, & \text{in } G \setminus \bar{D}, \\ \frac{\partial u^s}{\partial \nu} + ik\lambda(x)u^s = -\frac{\partial u^i}{\partial \nu} - ik\lambda(x)u^i, & \text{on } \partial D, \\ \frac{\partial u^s(x)}{\partial \nu} + \int_{\partial G} K(x, y)u^s(y)ds(y) = 0, & \text{on } \partial G \end{cases}$$

with kernel K defined by $K(\theta - \theta') := -\frac{k}{\pi} \sum_{n=0}^{\infty} \frac{H_n^{(1)'}(kR_0)}{H_n^{(1)}(kR_0)} \cos n(\theta - \theta')$. Then the inverse problem can be stated as: identify $(\partial D, \lambda(x))$ using $u^s(x)|_{\partial G}$.

For this problem, we express the solution $u^s(x)$ to PDE in terms of the combination of fundamental solution $\Phi(x, z_j)$ with source points outside of the domain $G \setminus \bar{D}$. Both the combination coefficients and the locations of point sources as well as $(\partial D, \lambda(x))$ are considered as the unknowns. Then we construct a nonlinear cost function in finite dimensional space with the discretization of $(\partial D, \lambda(x))$ and some regularizing terms. The approximation to $(\partial D, \lambda(x))$ is defined as the minimizer to the cost function. The existence and the convergence property of the minimizer are proven. Numerical tests have shown that this method is valid.

References

[1] T. Arens, *Why linear sampling works*, Inverse Problems, **20(1)** (2004), 163–173.

[2] F. Cakoni, D. Colton, P.Monk, *The Linear Sampling Method in Inverse Electromagnetic Scattering*, CCBMS-NSF Regional Conference Series in Applied Mathematics, **80**, (2011).

[3] D.L. Colton, R. Kress, *Inverse Acoustic and Electromagnetic Scattering Theory*, Springer-Verlag, Berlin, (1992).

[4] A. Karageorghis, D.Lesnic, *Application of the MFS to inverse obstacle scattering problems*, Engineering Analysis with Boundary Elements, **35(4)** (2011), 631–638.

[5] R. Kress, *Linear Integral Equations*, Springer-Verlag, Berlin, (1989).

[6] A. Kirsch, N. Grinberg, *The Factorization Method for Inverse Problems*, Oxford University Press, (2008).

[7] J.J. Liu, J. Cheng, G. Nakamura, *Reconstruction and uniqueness of an inverse scattering problem with impedance boundary*, Science in China Ser.A, **45(11)** (2002), 1408–1419.

[8] J.J. Liu, G. Nakamura, M. Sini, *Reconstruction of the shape and surface impedance from acoustic scattering data for arbitrary cylinder*, SIAM J. Applied Mathematics, **67(4)** (2007), 1124–1146.

[9] J.J. Liu, M. Sini, *On the accuracy of the numerical detection of complex obstacles from far field data using the probe method*, SIAM J. Scientific Computing, **31(4)** (2009), 2665–2687.

[10] H.B. Wang, J.J. Liu, *On the stability of Dirichlet-to-Neumann map in inverse scattering problems*, Science China Mathematics, **53(8)** (2010), 2069–2084.
[11] H.B. Wang, J.J. Liu, *Recovering the Dirichlet-to-Neumann map in inverse scattering problem using integral equation methods*, Advances in Computational Mathematics, **36(2)** (2011), 279–297.
[12] R. Potthast, Point Sources and Multipoles in Inverse Scattering Theory, Chapman & Hall/CRC, (2011).

Inverse Eddy Current Problems

BASTIAN HARRACH
(joint work with Lilian Arnold)

Transient excitation currents generate electromagnetic fields which, in turn, induce electric currents in proximal conductors. For slowly varying fields, this can be described by the eddy current equations, which are obtained by neglecting the dielectric displacement currents in Maxwell's equations (cf. [1])

$$(1) \qquad \partial_t(\sigma E) + \operatorname{curl}\left(\frac{1}{\mu} \operatorname{curl} E\right) = -\partial_t J \quad \text{in } \mathbb{R}^3 \times]0, T[.$$

The eddy current equations are of parabolic-elliptic type. In insulating regions ($\sigma(x) = 0$), the field instantaneously adapts to the excitation (quasistationary elliptic behaviour), while in conducting regions ($\sigma > 0$), this adaptation takes some time due to the induced eddy currents (parabolic behaviour).

The direct problem. The eddy current equations are often treated by separating the elliptic and the parabolic part. However, in view of studying inverse eddy current problems, it is desirable to formulate them in a *unified* way. In such a unified formulation σ should merely be a parameter, and it should be possible to differentiate solutions with respect to this parameter. In other words, a unified formulation should allow to characterize, e.g., *how the solution of an elliptic equation changes if the equation becomes a little bit parabolic.*

Let $\mu \in L_+^\infty(\mathbb{R}^3)$ and let $\sigma \in L^\infty(\mathbb{R}^3)$ be nonnegative and have bounded support Ω. Let $J_t \in L^2(0, T, W(\operatorname{curl}, \mathbb{R}^3)')$ be divergence free. The natural unified variational formulation of the eddy current equation is the following.

Natural variational formulation: Find $E \in L^2(0, T, W(\operatorname{curl}))$ that solves

$$\int_0^T \int_{\mathbb{R}^3} \left(\sigma E \cdot \partial_t \Phi - \frac{1}{\mu} \operatorname{curl} E \cdot \operatorname{curl} \Phi\right) = \int_0^T \int_{\mathbb{R}^3} J_t \cdot \Phi.$$

for all smooth Φ with $\Phi(\cdot, T) = 0$.

It can be shown that this formulation is indeed equivalent to solving (1) with zero initial conditions. The formulation can also easily be extended to include non-zero initial conditions on the support of σ, cf. [2]. This natural variational formulation is, however, not coercive with respect to the norm $||\cdot||_{L^2(0,T,W(\operatorname{curl}))}$. It is tempting to consider the following gauged formulation instead.

Gauged variational formulation: Find a *divergence-free* $E \in L^2(0, T, W(\mathrm{curl}))$ that solves

$$\int_0^T \int_{\mathbb{R}^3} \left(\sigma E \cdot \partial_t \Phi - \frac{1}{\mu} \mathrm{curl}\, E \cdot \mathrm{curl}\, \Phi \right) = \int_0^T \int_{\mathbb{R}^3} J_t \cdot \Phi.$$

for all smooth and *divergence-free* Φ with $\Phi(\cdot, T) = 0$.

This gauged formulation is coercive and thus solvable using the Lions-Lax-Milgram Theorem. However, the solution of this gauged formuation will, in general, not solve the original eddy current equation (1), not even after regauging it with a gradient field.

In [2], we propose a new, uniquely solvable and uniformly coercive variational formulation that determines the solution of the eddy current equation (1) up to the addition of a gradient field. Similarly to classical (A, φ)-formulations, we write

$$E = A + \nabla \varphi$$

with a divergence free field A and a gradient field $\nabla \varphi$. The crucial point is to consider $\nabla \varphi = \nabla \varphi_A$ as function of A by solving

$$\mathrm{div}\, \sigma \nabla \varphi_A = - \mathrm{div}\, \sigma A.$$

To ensure the solvability of this equation we require that $\sigma|_\Omega \in L^\infty_+(\Omega)$ where $\Omega := \mathrm{supp}\, \sigma \supset B_R(0)$ is a disjoint union of finitely many Lipschitz domains with connected complements. It is an open problem whether the mapping $A \mapsto \varphi_A$ can be defined for general non-negative $\sigma \in L^\infty(\mathbb{R}^3)$.

Unified variational formulation: Find a *divergence-free* $A \in L^2(0, T, W(\mathrm{curl}))$ that solves

$$\int_0^T \int_{\mathbb{R}^3} \left(\sigma(A + \nabla \varphi_A) \cdot \partial_t \Phi - \frac{1}{\mu} \mathrm{curl}\, A \cdot \mathrm{curl}\, \Phi \right) = \int_0^T \int_{\mathbb{R}^3} J_t \cdot \Phi.$$

for all smooth divergence-free Φ with $\Phi(\cdot, T) = 0$.

Theorem 1 (Thm. 3.2 in [2]). *The unified variational formulation is uniformly coercive with respect to σ. There exists a unique divergence-free solution $A \in L^2(0, T, W(\mathrm{curl}))$. $A + \nabla \varphi_A$ is one solution of the eddy-current equation and every other solution E of the eddy current equation fulfills*

$$\mathrm{curl}\, E = \mathrm{curl}\, A \quad and \quad \sqrt{\sigma} E = \sqrt{\sigma}(A + \nabla \varphi).$$

Also, the unified formulation allows us to rigorously linearize E w.r.t. σ around $\sigma_0 = 0$, see again [2].

The inverse problem. Let us now turn to the inverse problem of determining $\Omega = \mathrm{supp}\, \sigma$ from electromagnetic measurements. A natural model for idealistic measurements (see, e.g., [4]) is the operator

$$\Lambda_\sigma : L^2(0, T, TL^2_\diamond(S)) \to L^2(0, T, TL^2_\diamond(S)'), \quad J_t \mapsto \gamma_\tau E,$$

where E solves the homogeneous eddy current equation with $[\nu \times \mathrm{curl}\, E]_S = J_t$ on some smooth two-dimensional measurement surface S. Note that $TL^2_\diamond(S)' \cong TL^2(S)/TL^2_\diamond(S)^\perp$, so that Λ_σ is well-defined even though E is not unique.

We aim to apply linear sampling and factorization methods to the inverse problem of determining $\Omega = \operatorname{supp} \sigma$ from Λ_σ. To this end we introduce

- The difference to reference measurements $\Lambda := \Lambda_\sigma - \Lambda_0$ where $\Lambda_0 : J_t \mapsto \gamma_\tau E_0$, and E_0 solves the conductivity-free magnetostatic equation

$$\operatorname{curl} \operatorname{curl} E_0 = -J_t \quad \text{in } \mathbb{R}^3 \times]0, T[.$$

- The time-integration operator $I : E(\cdot, \cdot) \mapsto \int_0^T E(\cdot, t) \mathrm{d}t$.
- Singular test functions

$$G_{z,d}(x) := \operatorname{curl} \frac{d}{4\pi|x - z|}, \qquad x \in \mathbb{R}^3 \setminus \{z\}$$

Proceeding similarly to [3] we can prove the following results:

Theorem 2 (Linear sampling method for inverse eddy current problems). *For every point z below S and every direction $d \in \mathbb{R}^3$*

$$\gamma_\tau G_{z,d} \in \mathcal{R}(I\Lambda) \quad \Longrightarrow \quad z \in \Omega$$

Theorem 3 (Factorization method for inverse eddy current problems). *For every point z below S and every direction $d \in \mathbb{R}^3$*

$$\gamma_\tau G_{z,d} \in \mathcal{R}(I(\Lambda + \Lambda')^{1/2}) \quad \Longleftarrow \quad z \in \Omega$$

We also have a preliminary proof for the implication "$\Longrightarrow$" in theorem 3 but this has yet to be checked rigorously. The results show that the measurement Λ_σ determine the conductor $\Omega = \operatorname{supp} \sigma$ and allow a fast numerical implementation.

Beyond sampling and factorization methods (joint work with M. Ullrich). Linear sampling and factorization methods require the numerical implementation of a range test. For this task, no convergent regularization strategies in the sense that

$$R_\delta(\tilde{\Lambda}_\sigma) \to \chi_\Omega \quad \text{for } ||\tilde{\Lambda}_\sigma - \Lambda_\sigma|| < \delta \to 0$$

have been found yet (though [7] gives a first step in this direction).

For the related problem of electrical impedance tomography (EIT) this problem can be overcome by using *monotony methods*. Let Λ_σ denote the Neumann-to-Dirichlet-operator in EIT for the conductivity $\sigma = 1 + \chi_D$ with an unknown inclusion D. Under some assumptions we can show that (see [6] for a preliminary version of this result)

$$D = \bigcup \left\{ B \ : \ \Lambda_{1+\chi_B} \geq \Lambda_\sigma \right\} = \bigcup \left\{ B \ : \ \tfrac{1}{2}\Lambda'(1)\chi_B \geq \Lambda_\sigma - \Lambda_1 \right\}$$

where the second equality is based on the fact that linearizing the inverse EIT problem does not lead to shape errors (see [5]).

This shows that unknown inclusions can be found by monotony tests for which convergent implementations seem straight-forward. However, extensions of this results beyond the setting of EIT have yet to be done.

References

[1] H. Ammari, A. Buffa and J.-C. Nédélec, *A justification of eddy currents model for the Maxwell equations*, SIAM J. Appl. Math. **60** (2000), 1805–1823.

[2] L. Arnold and B. Harrach, *A unified variational formulation for the parabolic-elliptic eddy current equations*, to appear.

[3] F. Frühauf, B. Gebauer and O. Scherzer, *Detecting interfaces in a parabolic-elliptic problem from surface measurements*, SIAM J. Numer. Anal. **45** (2007), 810–836.

[4] B. Gebauer, M. Hanke and C. Schneider, *Sampling methods for low-frequency electromagnetic imaging*, Inverse Problems **24** (2008), 015007.

[5] B. Harrach and J. K. Seo, *Exact shape-reconstruction by one-step linearization in electrical impedance tomography*, SIAM J. Math. Anal. **42** (2010), 1505–1518.

[6] B. Harrach and M. Ullrich, *Monotony based imaging in EIT*, AIP Conf. Proc. **1281** (2010), 1975–1978.

[7] A. Lechleiter, *A regularization technique for the factorization method*, Inverse problems **22** (2006), 1605.

Inverse scattering of elastic waves by diffraction gratings
Johannes Elschner
(joint work with Guanghui Hu)

Diffraction phenomena for elastic waves propagating in unbounded periodic and non-periodic structures have many applications in geophysics and seismology. The talk presents recent work on the scattering of time-harmonic plane elastic waves by two-dimensional diffraction gratings with Lipschitz grating profiles. The first part gives an overview on existence and uniqueness results for the direct scattering problems, using a variational approach on a bounded periodic cell that involves the Dirichlet-to-Neumann map on the artificial boundary [4]. The approach can be extended to elastic scattering by rough surfaces [5] and biperiodic diffraction gratings in 3D [6]. Earlier solvability results for smooth profiles have been obtained in [1], [2], using integral equation methods.

Then the problem of recovering a two-dimensional elastic diffraction grating from measurements on a horizontal line above the structure is considered. We present global uniqueness results within the class of polygonal grating profiles by a minimal number of incident pressure or shear waves under the boundary conditions of the third and fourth kind [7]. In particular, using a reflection principle for the Navier equation, all unidentifiable polygonal grating profiles that correspond to only one given incident elastic field can be completely classified. The case of the first kind boundary conditions (Dirichlet problem) remains open because of the lack of a corresponding reflection principle. Generalizations to biperiodic polyhedral diffraction gratings are also mentioned [8].

The last part of the talk is devoted to a reconstruction method applied to the inverse Dirichlet problem for the two-dimensional quasi-periodic Navier equation. To reconstruct the profile curve of an elastic diffraction grating from near and far field data, this highly ill-posed problem is reformulated as a nonlinear optimization problem, following an approach first developed by Kirsch and Kress in the case of

inverse acoustic obstacle scattering; see [3]. The optimization method combined with Tikhonov regularization is applied to smooth and piecewise linear gratings, leading to satisfactory numerical reconstructions from exact and noisy data [9].

References

[1] T. Arens, *The scattering of plane elastic waves by a one-dimensional periodic surface*, Math. Meth. Appl. Sci. **22** (1999), 55–72.

[2] T. Arens, *Existence of solution in elastic wave scattering by unbounded rough surfaces*, Math. Meth. Appl. Sci. **25** (2002), 507–528.

[3] D. Colton and R. Kress, *Inverse Acoustic and Electromagnetic Scattering Theory*, Applied Mathematical Sciences, Vol. **93**, Springer-Verlag, Berlin, 1992.

[4] J. Elschner and G. Hu, *Variational approach to scattering of plane elastic waves by diffraction gratings*, Math. Meth. Appl. Sci. **33** (2010), 1924–1941.

[5] J. Elschner and G. Hu, *Scattering of plane elastic waves by three-dimensional diffraction gratings*, Math. Models Methods Appl. Sci. **22** (2012), 1150019/1-34.

[6] J. Elschner and G. Hu, *Elastic scattering by unbounded rough surfaces*, WIAS Preprint No. 1677, 2012.

[7] J. Elschner and G. Hu, *Inverse scattering of elastic waves by periodic structures: uniqueness under the third or fourth kind boundary conditions*, Meth. Appl. Anal. **18** (2011) 215-244.

[8] J. Elschner and G. Hu, *Uniqueness in inverse scattering of elastic waves by three-dimensional polyhedral diffraction gratings*, J. Inverse Ill-Posed Probl. **19** (2011) 717-768.

[9] J. Elschner and G. Hu, *An optimization method in inverse elastic scattering for one-dimensional grating profiles*, WIAS Preprint No. 1622, 2011.

An Inverse Problem for a Waveguide

Peter Monk

(joint work with Virginia Selgas)

We suggest the use of the Gap Reciprocity Method (RGM) of Colton and Haddar [2] to detect partial blockages in a waveguide using multistatic acoustic scattering measurements at a single frequency. Our intended application is to the remote inspection of buried pipes such as sewers. The waveguide is modeled as an infinite cylinder with sound hard boundary conditions, and sound propagation is governed by the Helmholtz equation. This work relies heavily on [1], but unlike [1] where the scatterer is sound soft and away from the walls of the waveguide, we consider a partial blockage represented by a penetrable scatter that can touch the walls.

The analysis of the RGM rests on understanding a novel interior transmission problem (ITP) featuring mixed boundary conditions (Neumann on part of the boundary of the scatterer and of interior transmission type on the remainder). In particular we need to know that this problem is well posed for almost all wave numbers. Following the ideas of [4], we can approach the analysis by writing the ITP as a fourth order problem and recognizing that a natural boundary condition completes the description of the mixed ITP. We prove in particular that, if they arise, interior transmission eigenvalues form at most a discrete set.

Using a single layer representation in the RGM we show that the method is a generalized Linear Sampling Method (LSM) [3] in which measurement and source points are on disjoint sets, and hence that the usual theorems concerning the blowup of solutions of the RGM equation can be proved. Thus we expect that the boundary of a partial blockage can detected by the blowup of the the RGM indicator function. Note that the RGM is to be preferred over the standard LSM in this case because the RGM allows us to isolate the part of the waveguide under study from the rest of the pipe (which might also include a manhole where the measuring instruments are deployed and that would need modeling in the LSM).

To test this theory we generate synthetic scattering data for several partial obstacles in a circular cylinder (both penetrable and sound hard - although the sound hard case is not covered by our theory). In each case the RGM is seen to detect the obstacles, and to provided rough images of the blockages, using data measured at a distance of approximately 30 pipe diameters from the blockage.

We have also tested one case in which the algorithm failed (a case not covered by our theory). We attempted to detect the sound hard end of a semi-infinite wave-guide using distant measurements. The RGM completely failed to detect the end of the fully blocked pipe. Using near field measurements the RGM did detect the blockage indicating that evanescent modes are needed in this case.

In future work we plan to investigate, and if possible characterize, the scatterers that cannot be detected by the method, and hope to find ways to detect these anomalous cases from the same data by other means.

REFERENCES

[1] L. BOURGEOIS AND E. LUNÉVILLE, *The linear sampling method in a waveguide: a modal formulation*, Inv. Prob., 24 (2008), pp. 15–8.

[2] D. COLTON AND H. HADDAR, *An application of the reciprocity gap functional to inverse scattering theory*, Inv. Prob., 21 (2005), pp. 383–98.

[3] D. COLTON AND A. KIRSCH, *A simple method for solving inverse scattering problems in the resonance region*, Inv. Prob., 12 (1996), pp. 383–93.

[4] D. COLTON, L. PAEIVAERINTA, AND J. SYLVESTER, *The interior transmission problem*, Inverse Problems and Imaging, 1 (2007), pp. 13–28.

Transmission Eigenvalues in One Dimension

JOHN SYLVESTER

The scattering operator for the tome harmonic Helmholtz equation maps the asympotics of incident waves (Herglotz wavefunctions) v_0 to the asymptotics of (outgoing) scattered waves u^+. The scatterer means the domain D, together with an index of refraction $n(x)$ supported in D.

$$\left(\Delta + k^2 n^2\right) u^+ = (1 - n^2)k^2 v_0$$
$$\left(\Delta + k^2\right) v_0 = 0$$

If the scattering operator has a zero eigenvalue, we say that k^2 is a transmission eigenvalue. It follows form Rellich's theorem and unique continuation that the scattered wave u^+ is identically zero outside D, and therefore that k^2 is an interior transmission eigenvalue for the pair (D, m), i.e.

$$\left(\Delta + k^2 n^2\right) u = (1 - n^2)k^2 v$$
$$\left(\Delta + k^2\right) v = 0$$
$$u\Big|_{\partial D} = 0 \qquad \frac{\partial u}{\partial \nu}\Big|_{\partial D}$$

The analogous interior problem for obstacle scattering is the Dirichlet problem, and the Dirichlet eigenvalues are fairly well understood. In particular, the Dirichlet eigenvalues of a one dimensional interval of length L are exactly $\frac{n^2\pi^2}{L^2}$. The one dimensional interior transmission eigenvalue problem, even for a constant index of refraction, is not as simple. In one dimension, the interior transmission equations become

$$u'' + k^2\sigma^2 u = k^2\sigma^2 v$$
$$v'' + k^2 v = 0$$
$$u(-\tfrac{L}{2}) = u(\tfrac{L}{2}) = 0 \qquad u'(-\tfrac{L}{2}) = u'(\tfrac{L}{2}) = 0$$

The (odd/even) solutions to this pair of constant coefficient ODE's correspond to the complex numbers k that solve the equations:

$$\frac{\sin\frac{kL(\sigma+1)}{2}}{\sigma + 1} = \pm\frac{\sin\frac{kL(\sigma-1)}{2}}{\sigma - 1}$$

and the two theorems below describe those k's .

Theorem 4. *If k is an interior transmission eigenvalue*

$$Im(k) \leq \frac{1}{2L}\log\frac{3\sigma + 1}{\sigma - 1}$$

Theorem 5. *Suppose that $\sigma > 1$, let $M = \frac{\sigma+1}{\sigma-1}$, and let $j \in \mathbb{Z}$*

  (1) *If $\frac{j}{M} \notin \mathbb{Z}$ and $\frac{j+1}{M} \notin \mathbb{Z}$, there are exactly two simple roots in the strip*

$$\frac{2j\pi}{(\sigma + 1)L} < Re(k) < \frac{2(j + 1)\pi}{(\sigma + 1)L}$$

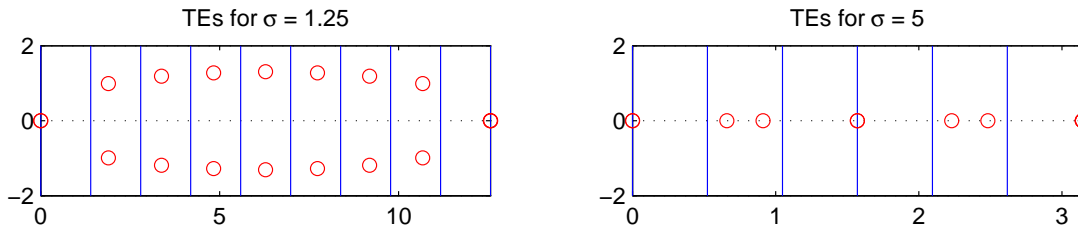 (a) *If $\lfloor\frac{j}{M}\rfloor \neq \lfloor\frac{j+1}{M}\rfloor$, both roots are real*
  (b) *ElseIf $\lfloor\frac{j}{M}\rfloor = \lfloor\frac{j+1}{M}\rfloor$ the roots are non-real complex conjugates*
  (2) *If $\frac{j}{M} \in \mathbb{Z}$, there is a quadruple root at $k = \frac{j}{M}$ and no other roots in the strip*

$$\frac{2(j - 1)\pi}{(\sigma + 1)L} < Re(k) < \frac{2(j + 1)\pi}{(\sigma + 1)L}$$

The transmission eigenvalues for two σ's, with $L = 2$, are plotted below. The vertical blue lines indicate the sets $Re(k) = \frac{2j\pi}{(\sigma+1)L}$. The roots that fall on these lines are quadruple.

REFERENCES

[1] A. Kirsch, *The denseness of the far field patterns for the transmission problem*, IMA J. Appl. Math., 37(3) (1986), pp. 213–225.

[2] D. Colton and P. Monk, *The inverse scattering problem for time-harmonic acoustic waves in an inhomogeneous medium*, Quart. J. Mech. Appl. Math., 41(1) (1988), pp. 97–125.

[3] D. Colton, A. Kirsch, and L. Päivärinta, *Far-field patterns for acoustic waves in an inhomogeneous medium*, SIAM J. Math. Anal., 20(6) (1989), pp. 1472–1483.

[4] L. Päivärinta and J. Sylvester, *Transmission eigenvalues*, SIAM J. Math. Anal., 40(2) (2008), pp. 738–753.

[5] D. Colton, L. Päivärinta, and J. Sylvester, *The interior transmission problem*, Inverse Probl. Imaging, 1(1) (2007), pp. 13–28.

[6] F. Cakoni, D. Gintides and Houssem Haddar, *The existence of an infinite discrete set of transmission eigenvalues*, SIAM J. Math. Anal., 42(1) (2010), pp. 237–255.

[7] J. Sylvester, *Discreteness of transmission eigenvalues via upper triangular compact operators*, SIAM J. Math. Anal., to appear.

[8] Y.-J. Leung and D. Colton, *Complex transmission eigenvalues for spherically stratified media*, preprint.

Solving an inverse scattering problem in the time domain by using the iterative time-reversal control method

Lauri Oksanen

The inverse problem of reconstructing an obstacle from measurements of acoustic waves in the time domain has attracted recent interest [5, 6, 7, 9, 10]. Here we consider a solution approach based on the boundary control (BC) method [8].

By using the BC method, a smooth wave speed can be fully reconstructed from the Neumann-to-Dirichlet operator. This uniqueness result is by Belishev [1], see also [2] for the anisotropic case. However, the BC method in its original form is unstable and seems to be hard to regularize. To remedy this, a computationally more feasible version of the BC method called the iterative time-reversal control (ITRC) method was introduced in [3].

In [11] we introduced a modification of the ITRC method and showed that it can reconstruct a convex penetrable obstacle in dimension two. Here we consider the case of a sound hard obstacle in arbitrary dimension and present some numerical simulations.

Our method locates the obstacle by computing the travel time distance to it from each point on the measurement boundary. Let us next describe this in detail. Let $M \subset \mathbb{R}^n$ be a compact domain with smooth boundary ∂M and let c be a smooth function on M that is bounded and bounded away from zero. Let $\Sigma \subset M^{\text{int}}$ be a compact set with nonempty interior and smooth boundary. Moreover, let $\Gamma \subset \partial M$ be open and $T > 0$. We model the measurements by the Neumann-to-Dirichlet operator,

$$\Lambda_{2T,\Gamma} : f \mapsto u^f|_{(0,2T) \times \Gamma}, \quad f \in C_0^\infty((0,T) \times \Gamma),$$

where $u = u^f$ is the solution of the wave equation,

$$
\begin{aligned}
\partial_t^2 u(t,x) - c(x)^2 \Delta u(t,x) &= 0, & (t,x) &\in (0,\infty) \times (M \setminus \Sigma), \\
\partial_\nu u(t,x) &= f(t,x), & (t,x) &\in (0,\infty) \times \partial M, \\
\partial_\nu u(t,x) &= 0, & (t,x) &\in (0,\infty) \times \partial\Sigma, \\
u|_{t=0}(x) = 0, \quad \partial_t u|_{t=0}(x) &= 0, & x &\in M \setminus \Sigma.
\end{aligned}
$$

We consider the inverse obstacle problem to obtain information on Σ given the measurements $\Lambda_{2T,\Gamma}$. For $x, y \in M$, we define the travel time distance $d(x,y)$ as the Riemannian distance with respect to the metric tensor $c(x)^{-2}dx^2$. Our method can reconstruct the distance $d(y,\Sigma)$ for $y \in \Gamma$ if $d(y,\Sigma) < T$. The method is based on the following two observations:

1. For a function $\tau \in C(\overline{\Gamma})$ satisfying $0 \leq \tau \leq T$ pointwise, the volume $V(M_\Sigma(\tau))$ of the *domain of influence* on $(M \setminus \Sigma, g)$,

   $$M_\Sigma(\tau) := \{x \in M \setminus \Sigma; \text{ there is } y \in \overline{\Gamma} \text{ s.t. } d_{M \setminus \Sigma}(x,y) \leq \tau(y)\},$$

   can be computed from $\Lambda_{2T,\Gamma}$ by solving a sequence of linear equations on $L^2((0,2T) \times \partial M)$.

2. For a function $\tau \in C(\overline{\Gamma})$, we have $M(\tau)^{\text{int}} \cap \Sigma^{\text{int}} \neq \emptyset$ if and only if

   $$V(M_\Sigma(\tau)) < V(M(\tau)),$$

   where $M(\tau)$ is a domain of influence on (M,g), that is,

   $$M(\tau) := \{x \in M; \text{ there is } y \in \overline{\Gamma} \text{ s.t. } d(x,y) \leq \tau(y)\}.$$

The volume V above refers to the Riemannian volume on (M,g) and $d_{M \setminus \Sigma}$ denotes the Riemannian distance on $(M \setminus \Sigma, g)$. See [12] for a proof of 1 and [13] for a proof of 2.

If the background wave speed c is known and $T > 0$ is large enough, then we can determine the distances $d(y,\Sigma)$, $y \in \Gamma$, by comparing the reconstructed volumes $V(M_\Sigma(\tau_{r,y}))$ with the background volumes $V(M(\tau_{r,y}))$ where

$$\tau_{r,y}(y') \approx \begin{cases} r, & y' = y, \\ 0, & \text{otherwise,} \end{cases} \quad r > 0, \ y \in \Gamma.$$

Thus we can visualize the set,

$$M \setminus \bigcup_{y \in \Gamma} \{x \in M; \ d(y,x) < d(y,\Sigma)\},$$

containing Σ. If $c = 1$ identically and $\Gamma = \partial M$ then this set is contained in the convex hull of Σ. In [11] we give also a uniqueness result without assuming that the background wave speed c is known.

We will next describe numerical simulations in the case that M is the unit square in $\mathbb{R}^2$, $c = 1$ identically and Σ is the disk with with radius 0.3 and center coinciding with the center of the unit square. In particular, we consider the case that $T \geq 1/2$ and Γ is the left edge of M, and define

$$\tau_r(y) = \begin{cases} r, & y \in \Gamma, \\ 0, & \text{otherwise,} \end{cases} \qquad r \in [0, 1/2].$$

We compute an approximation of the volume $V(M_\Sigma(\tau_r))$ by constructing a wave source $f \in L^2((T-r, T) \times \Gamma)$ such that the corresponding solution u^f satisfies

$$\left\| u^f(T) \right\|_{L^2(M;dV)}^2 \approx \left\| 1_{M_\Sigma(\tau_r)} \right\|_{L^2(M;dV)}^2 = V(M_\Sigma(\tau_r)).$$

The norm of $u^f(T)$ can be computed from the boundary data $\Lambda_{\Gamma,2T}$ by using Blagoveščenskiĭ's identity [4]. Moreover, the source f can be obtained from $\Lambda_{\Gamma,2T}$ by solving a linear equation on $L^2((T-r, T) \times \Gamma)$, see [12, Th. 2.1].

We discretize the problem by considering piecewise constant sources f that can be represented as a linear combination of the functions

$$f_j(t, x) := 1_{[0,h]}(t) 1_{\Gamma_j}(x), \quad j = 1, \dots, N,$$

and their time translations by an integer multiple of h. Here $h > 0$ is fixed and the sets Γ_j form a uniform partition of Γ. This corresponds to measuring the echoes of N square pulses on Γ. The small parameter h models the time resolution of the measurements. In Figure 1 we show numerical results with $N = 20$ and $h = 0.002$.

References

[1] M. I. Belishev. An approach to multidimensional inverse problems for the wave equation. *Dokl. Akad. Nauk SSSR*, 297(3):524–527, 1987.

[2] M. I. Belishev and Y. V. Kurylev. To the reconstruction of a Riemannian manifold via its spectral data (BC-method). *Comm. Partial Differential Equations*, 17(5-6):767–804, 1992.

[3] K. Bingham, Y. Kurylev, M. Lassas, and S. Siltanen. Iterative time-reversal control for inverse problems. *Inverse Probl. Imaging*, 2(1):63–81, 2008.

[4] A. S. Blagoveščenskiĭ. The inverse problem of the theory of seismic wave propagation. In *Problems of mathematical physics, No. 1: Spectral theory and wave processes (Russian)*, pages 68–81. (errata insert). Izdat. Leningrad. Univ., Leningrad, 1966.

[5] C. Burkard and R. Potthast. A time-domain probe method for three-dimensional rough surface reconstructions. *Inverse Probl. Imaging*, 3(2):259–274, 2009.

[6] Q. Chen, H. Haddar, A. Lechleiter, and P. Monk. A sampling method for inverse scattering in the time domain. *Inverse Problems*, 26(8):085001, 17, 2010.

[7] H. Haddar, A. Lechleiter. A Factorization Method for a Far-Field Inverse Scattering Problem in the Time Domain. *Comm. Partial Differential Equations* (to appear).

[8] A. Katchalov, Y. Kurylev, and M. Lassas. *Inverse boundary spectral problems*, volume 123 of *Chapman & Hall/CRC Monographs and Surveys in Pure and Applied Mathematics*. Chapman & Hall/CRC, Boca Raton, FL, 2001.

[9] C. D. Lines and S. N. Chandler-Wilde. A time domain point source method for inverse scattering by rough surfaces. *Computing*, 75(2-3):157–180, 2005.
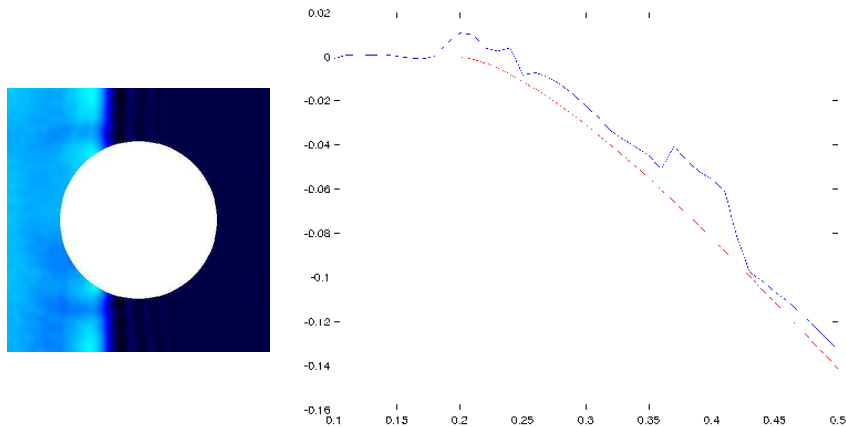
FIGURE 1. *On left.* The solution $u^f(T) \approx 1_{M_\Sigma(\tau_r)}$ constructed using only $\Lambda_{\Gamma,2T}$. Here $r = 0.4$. *On right.* Reconstruction from noisy $\Lambda_{\Gamma,2T}$. Signal-to-noise ratio is 7 dB. The approximated difference in the volumes, $\|u^f(T)\| - V(M(r))$, as a function of r (blue) and the true difference $V(M_\Sigma(\tau_r)) - V(M(r))$ (dashed red). An approximation for the distance $\min_{y \in \Gamma} d(y, \Sigma) = 0.2$ is obtained by looking when the blue curve drops below zero.

[10] D. R. Luke and R. Potthast. The point source method for inverse scattering in the time domain. *Math. Methods Appl. Sci.*, 29(13):1501–1521, 2006.
[11] L. Oksanen. Inverse obstacle problem for the non-stationary wave equation with an unknown background. arXiv:1106.3204, June 2011.
[12] L. Oksanen. Solving an inverse problem for the wave equation by using a minimization algorithm and time-reversed measurements. *Inverse Probl. Imaging*, 5(3):731–744, 2011.
[13] L. Oksanen. Solving an inverse obstacle problem for the wave equation by using the boundary control method. In preparation.

Inverse source problems for the Helmholtz equation and the windowed Fourier transform

ROLAND GRIESMAIER

(joint work with Martin Hanke and Thorsten Raasch)

We consider the following inverse source problem for acoustic or electromagnetic wave propagation at a fixed frequency:

> *Given the radiated far field pattern of a solution to the Helmholtz equation corresponding to a compactly supported source, recover information on the support of the source.*

This problem has been widely studied and is well-known to be ill-posed, see, e.g., Isakov [5]; without additional assumptions on the source it does not even have a unique solution. For this reason Kusiak and Sylvester [6, 9] recently introduced generalized notions of solution, such as the so-called *convex scattering support*. This is the smallest convex set $\mathscr{C}$ such that for every neighborhood of $\mathscr{C}$ there

exists a source supported in this neighborhood that radiates the given far field. The convex scattering support is uniquely determined by the far field.

We present a new numerical reconstruction method for this inverse problem that not only gives a reasonable approximation of the convex scattering support but also seems to provide information about the number and the relative locations of individual sources. This method relies on a local analysis of the far field by means of the windowed Fourier transform combined with the classical filtered backprojection algorithm (see, e.g., Natterer [7]). Earlier works with related view points are, e.g., [1, 3].

To be more specific, let $f \in \mathscr{E}'(\mathbb{R}^2)$ be a compactly supported *source* such that $\operatorname{supp} f \subset B_R(0)^1$, $R > 0$, and consider a fixed *wave number* $\kappa > 0$. The corresponding *field radiated by* f is the solution of the Helmholtz equation

$$-\Delta u - \kappa^2 u = f \qquad \text{in } \mathbb{R}^2$$

together with the Sommerfeld radiation condition at infinity (see, e.g., Colton and Kress [2]). Writing u in terms of the fundamental solution to the Helmholtz equation it follows immediately that the radiated field has the asymptotic behavior

$$u(x) = \frac{e^{i\pi/4}}{\sqrt{8\pi}} \frac{e^{i\kappa|x|}}{\sqrt{\kappa|x|}} u^\infty(\widehat{x}) + \mathcal{O}(|x|^{-3/2}) \qquad \text{for } |x| \to \infty,$$

where $\widehat{x} := x/|x| \in S^1$. The *far field* u^∞ *radiated by* f is given by $u^\infty(\widehat{x}) = \widehat{f}(\kappa\widehat{x})$, $\widehat{x} \in S^1$, i.e., it coincides with the Fourier transform of f evaluated on κS^1.

Now let $\varepsilon > 0$ and

$$\chi_\varepsilon(t) = \frac{1}{\sqrt{2\pi}\varepsilon} e^{-\frac{1}{2}t^2/\varepsilon^2}, \qquad t \in \mathbb{R},$$

be a one-dimensional Gaussian *window function* with standard deviation ε. Using polar coordinates for $\theta = (\cos\vartheta, \sin\vartheta) \in S^1$ and $\widehat{x}_t = (\cos t, \sin t) \in S^1$ with $\vartheta, t \in \mathbb{R}$, the *windowed Fourier transform* of the far field u^∞ is defined to be

$$(S_\varepsilon u^\infty)(\theta, \omega) := \int_{-\infty}^{\infty} e^{-i\omega t} \chi_\varepsilon(t) u^\infty(\widehat{x}_{\vartheta+t}) \, dt$$

for $\theta \in S^1$ and $\omega \in \mathbb{R}$.

Assuming that the source f is a distribution of order zero, and denoting by $|f|_{\mathrm{TV}}$ its total variation in terms of measures, it has been observed in [4] that the windowed Fourier transform of the far field radiated by f satisfies

$$(1) \qquad (S_\varepsilon u^\infty)(\theta, \omega) = \big(T_{i\kappa}(g_\varepsilon * f)\big)\Big(\theta^\perp, -\frac{\omega}{\kappa}\Big) + \mathcal{O}\big(\kappa R\varepsilon^2|f|_{\mathrm{TV}}\big).$$

Here

$$g_\varepsilon(x) := \frac{\varepsilon\kappa}{\sqrt{2\pi}} e^{1/(2\varepsilon^2)} e^{-\frac{1}{2}|x|^2\varepsilon^2\kappa^2}, \qquad x \in \mathbb{R}^2,$$

---

^{1}Here $B_R(0)$ denotes the ball of radius R around the origin.

is a rescaled two-dimensional Gaussian with standard deviation $1/(\varepsilon\kappa)$, and $T_{\mathrm{i}\kappa}$ denotes the *exponential Radon transform* with purely imaginary exponent $\mathrm{i}\kappa$, which is defined to be

$$
\big(T_{\mathrm{i}\kappa}h\big)(\phi,s) := \int_{x\cdot\phi=s} e^{\mathrm{i}\kappa x\cdot\phi^\perp} h(x)\,\mathrm{d}x = \int_{-\infty}^{\infty} e^{\mathrm{i}\kappa t} h(s\phi + t\phi^\perp)\,\mathrm{d}t\,,
$$

cf., e.g., [7, p. 47]. So, assuming $\varepsilon > 0$ is sufficiently small, the windowed Fourier transform of the far field can be considered as an approximation of the exponential Radon transform of a smooth mollification of the source.

This suggests a means to deduce information about the unknown source from the given far field: First, one computes the windowed Fourier transform of the far field choosing ε sufficiently small, then rescales the result according to the right hand side of (1), and finally inverts the exponential radon transform $T_{\mathrm{i}\kappa}$ to obtain a mollified version of f. However, although there do exist explicit inversion formulas for $T_{\mathrm{i}\kappa}$, see, e.g., You [10], its inversion is severely ill-posed, cf. Natterer [8].

Therefore we follow a different approach by observing that for a single point source $f = \delta_z$ located in $z = r(\cos\varphi, \sin\varphi) \in \mathbb{R}^2$ the exponential Radon transform of this source is given by

$$
\big(T_{\mathrm{i}\kappa}\delta_z\big)(\theta,s) = e^{\mathrm{i}\kappa z\cdot\theta^\perp}\delta(s - z\cdot\theta)\,,
$$

i.e., its support is the graph of the function $\theta \mapsto s = z\cdot\theta = r\cos(\vartheta - \varphi)$. Accordingly, the windowed Fourier transform of its far field satisfies

$$
\big(S_\varepsilon u^\infty\big)(-\theta^\perp, -s\kappa) \approx e^{\mathrm{i}\kappa z\cdot\theta^\perp} e^{-\frac{1}{2}\varepsilon^2\kappa^2(s-z\cdot\theta)^2}\,,
$$

and thus

$$
(2)\qquad\qquad \big|\big(S_\varepsilon u^\infty\big)(-\theta^\perp, -s\kappa)\big| \approx \big(R(g_\varepsilon * f)\big)(\theta,s)\,,
$$

where the right-hand side denotes the classical Radon transform of $g_\varepsilon * f$. As a consequence, we can compute a mollified approximation $g_\varepsilon * f$ of the point source by applying the inverse Radon transform to the left-hand side of (2). Numerically this procedure not only works for single point scatterers but also for superpositions of sources.

To illustrate our findings we consider a collection of four point sources $f = c_1\delta_{z_1} + c_2\delta_{z_2} + c_3\delta_{z_3} + c_4\delta_{z_4}$ located at $z_1 = (4,4)$, $z_2 = (-2,8)$, $z_3 = (4,-8)$ and $z_4 = (-2,-1)$ with "strengths" $c_1 = 1 - \mathrm{i}$, $c_2 = 1$, $c_3 = -1$ and $c_4 = 1 + \mathrm{i}$. We choose $\kappa = 10$ and use $\varepsilon = \pi/18$ in the windowed Fourier transform. The left hand side of Figure 1 shows absolute values of the windowed Fourier transform $|(S_\varepsilon u^\infty)(-\theta^\perp, -s\kappa)|$ as a color coded plot, where the polar angle ϑ of $\theta \in S^1$ varies along the horizontal axis and s along the vertical axis. The right-hand side is the result of the filtered backprojection algorithm with these data, which looks like three slightly distorted Gaussians centered at the sources z_1, z_2, z_3 and z_4.

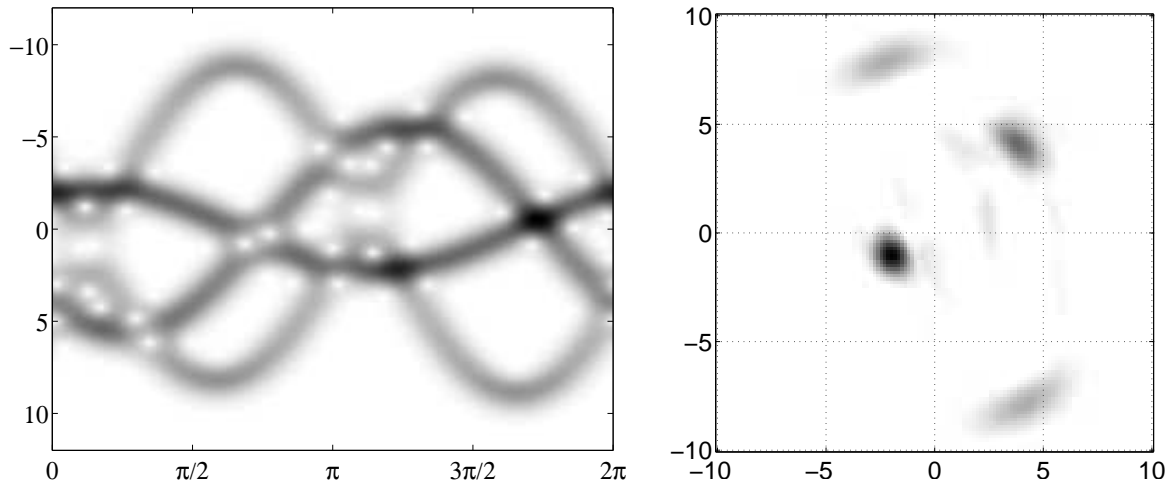A complete derivation of these results including more numerical reconstructions can be found in [4].

FIGURE 1. *Left:* Approximation of the Radon transform. *Right:* Reconstruction with filtered backprojection

REFERENCES

[1] O. M. Bucci, A. Capozzoli, and G. D'Elia, *Determination of the convex hull of radiating or scattering systems: a new, simple and effective approach*, Inverse Problems **18** (2002), 1621-1638.

[2] D. Colton and R. Kress, *Inverse Acoustic and Electromagnetic Scattering Theory*, 2nd ed., Springer, Berlin, 1998.

[3] A. J. Devaney, *Reconstructive tomography with diffracting wavefields*, Inverse Problems **2** (1986), 161–183.

[4] R. Griesmaier, M. Hanke, and T. Raasch, *Inverse source problems for the Helmholtz equation and the windowed Fourier transform*, submitted.

[5] V. Isakov, *Inverse Source Problems*, Amer. Math. Soc., Providence, 1990.

[6] S. Kusiak and J. Sylvester, *The scattering support*, Comm. Pure Appl. Math. **56** (2003), 1525–1548.

[7] F. Natterer, *The Mathematics of Computerized Tomography*, Teubner, New York, 1986.

[8] F. Natterer, *The attenuated Radon transform for complex attenuation*, manuscript, 2007.

[9] J. Sylvester, *Notions of support for far fields*, Inverse Problems **22** (2006), 1273–1288.

[10] J. You, *The attenuated Radon transform with complex coefficients*, Inverse Problems **23** (2007), 1963–1971.

Inverse Problems in Local Helioseismology

THORSTEN HOHAGE

(joint work with Laurent Gizon)

The aim of local helioseismology is to compute three-dimensional reconstructions of flow velocities and other physical quantities in the Solar interior from high resolution Doppler-shift data of the line-of-sight velocities

$$\phi(\mathbf{r}, t) := \widehat{\mathbf{l}} \cdot \mathbf{v}(\mathbf{r}, t)$$

on the Sun's surface. Here $\widehat{\mathbf{l}}$ denotes the line of sight unit vector, and $\mathbf{v}(\mathbf{r}, t)$ the velocity at position $\mathbf{r}$ and time t. Such data have been collected since 1995 by the

ground based **G**lobal **O**scillations **N**etwork **G**roup (GONG) and by the **M**ichelson **D**oppler **I**mager (MDI) on board of the **So**lar and **H**eliospheric **O**bservatory (SOHO) launched 1995. In February 2010 the Solar Dynamics Observatory (SDO) has been launched which collects more than 1TB of Doppler-shift data of the Sun's surface velocity each day.

Duvall et al. [1] proposed to determine background flow velocities $\mathbf{v}_0$ in the convection zone of the Sun by shifts of travel times of acoustic waves with respect to the standard Solar model. They suggested to determine such travel time shifts using correlations of the form

$$C(\mathbf{r}_1, \mathbf{r}_2, t) := \int_0^T \phi(\mathbf{r}_1, \tilde{t}) \phi(\mathbf{r}_2, \tilde{t} + t) \, d\tilde{t} \,.$$

The derivation of the corresponding forward problem can be summarized as follows (see [2]): The displacements $\boldsymbol{\xi}(\mathbf{r}, t)$ of solar waves satisfy a wave equation $\mathcal{L}[\mathbf{v}_0]\boldsymbol{\xi} = \mathbf{S}$ in which the unknown background velocities $\mathbf{v}_0$ appear as parameters. The sources $\mathbf{S}$, which are caused by turbulent convection, are modeled as a random process. If $(\mathcal{O}\boldsymbol{\xi})(\mathbf{r}, t) := \widehat{\mathbf{l}} \cdot \partial_t \boldsymbol{\xi}(\mathbf{r}, z, t)$ is defined such that $\phi = \mathcal{O}\mathcal{L}[v_0]^{-1}\mathbf{S}$, then the covariance operators of $\mathbf{S}$ and ϕ are related by

$$\mathbf{Cov}_\phi[\mathbf{v}_0] = \mathcal{O}\mathcal{L}[\mathbf{v}_0]^{-1}\mathbf{Cov_S}\mathcal{L}[\mathbf{v}_0]^{-*}\mathcal{O}^* \,.$$

The covariance operator $\mathbf{Cov}_\phi[\mathbf{v}_0]$ can be estimated by the integral operator

$$\left(\widehat{\mathbf{Cov}_\phi}[\mathbf{v}_0] w \right)(\mathbf{r}_1, t) := \int \int C(\mathbf{r}_1, \mathbf{r}_2, t_2 - t_1) w(\mathbf{r}_2) \, d\mathbf{r}_2 \, dt_2 \,.$$

Usually the signal-to-noise ratio of the point-to-point correlations $C(\mathbf{r}_1, \mathbf{r}_2, t)$ is too small. In principle, the signal-to-noise ratio can be made arbitrarily large by increasing the averaging time T, however T cannot be chosen too large to avoid motion blur. To improve the signal-to-noise ratio and to reduce the length of the right hand side vector of the inverse problem, certain space-time averages of the form

$$\widehat{\tau}_\alpha(\mathbf{r}_1) = \left(\widehat{\mathbf{Cov}_\phi}[\mathbf{v}_0] w_\alpha(\cdot - \mathbf{r}_1) \right)(\mathbf{r}_1, 0) = \int \int C(\mathbf{r}_1, \mathbf{r}_1 + \mathbf{r}_2, t) w_\alpha(\mathbf{r}_2, t) \, d\mathbf{r}_2 \, dt$$

are computed. The weights w_α are chosen such that $\tau_\alpha(\mathbf{r}_1)$ indicates some travel time of a wave starting at $\mathbf{r}_1$, e.g. an average point-to-annulus travel time.

We approximate $\mathbf{Cov}_\phi[\mathbf{v}_0] \approx \mathbf{Cov}_\phi[0] + \mathbf{Cov}'_\phi[0]\mathbf{v}_0$ by its first order Taylor approximation. On an approximately planar patch of the Sun's surface there are *sensitivity kernels* $K_{\alpha,\beta}$ such that

$$\left((\mathbf{Cov}'_\phi[0]\mathbf{v}_0) w_\alpha(\cdot - \mathbf{r}_1) \right)(\mathbf{r}_1, 0) = \sum_\beta \int \int_{-z_0}^0 K_{\alpha\beta}(\mathbf{r}_1 - \mathbf{r}_2, z) v_{0,\beta}(\mathbf{r}_2, z) \, d\mathbf{r}_2 \, dz \,.$$

Then the estimated travel time shifts $\delta\widehat{\tau}_\alpha := \widehat{\tau}_\alpha - \mathbf{Cov}_\phi[\mathbf{v}_0] w_\alpha(\cdot, 0)$ satisfy the equation

$$(1) \qquad (\delta\widehat{\tau}_\alpha)(\mathbf{r}_1) = \int \int_{-z_0}^0 \sum_\beta K_{\alpha\beta}(\mathbf{r}_1 - \mathbf{r}_2, z) v_{0,\beta}(\mathbf{r}_2, z) \, d\mathbf{r}_2 \, dz + n_\alpha(\mathbf{r}_1) \,.$$

The covariance kernel

$$\Lambda_{\alpha\alpha'}(\mathbf{r}_2) := \mathbb{E}\left[n_\alpha(\mathbf{r}_1)n_{\alpha'}(\mathbf{r}_1 + \mathbf{r}_2)\right]$$

of the noise can be estimated from the case $\mathbf{v}_0 = 0$ (see [3]).

The system of equations (1) is a *linear statistical inverse problem*

$$\delta\tau = \mathbf{K}\mathbf{v}_0 + \mathbf{n}$$

of a very nice structure: After discretization of the z variable, it has the form of a *system of convolution equations* where $\mathbf{K}$ is a matrix of two-dimensional convolution operators with the sensitivity kernels $K_{\alpha,\beta}$ as convolution kernels. The covariance matrix of $\mathbf{n}$ is a full matrix, but it is invariant with respect to horizontal translations, and a good estimate is known. A typical size of the problem is a 240×267 system of convolution operators on a grid of 400^2 points resulting in about $4 \cdot 10^7$ unknowns.

Due to the assumed horizontal invariance, it is possible to compute a complete singular value decomposition (SVD) of the forward operator since it separates into a system of small SVDs for each spatial frequency. We show how the physical side constraint $\mathrm{div}\,(\rho\mathbf{v}_0) = 0$ with the density $\rho = \rho(z)$ can be incorporated in the inversion procedure. The special structure of the problem allows the use of Pinsker-type estimators, which are known to be optimal for statistical inverse problems among all linear estimators.

We show some results for real data and compare our method to the method of Subtractive Optimally Localized Averaging (SOLA), which can be seen as a version of the method of approximate inverse .

References

[1] T. L. Duvall Jr., S. M. Jefferies, J. W. Harvey, and M. A. Pomerantz. *Time-distance helioseismology.* Nature **362** (1993), 430–432.

[2] L. Gizon and A. C. Birch. Time-distance helioseismology: The forward problem for random distributed sources. The Astrophysical Journal **571** (2002), 966.

[3] L. Gizon and A. C. Birch. *Time-distance helioseismology: Noise estimation.* The Astrophysical Journal **6**14 (2004), 472.

[4] J. Jackiewicz, A. C. Birch, L. Gizon, S. Hanasoge, T. Hohage, J. B. Ruffio, and M. Svanda. Multichannel three-dimensional ola inversion for local helioseismology solar physics. Solar Phys **276** (2012), 19–33.

Conformal mapping and inverse scattring

Rainer Kress

(joint work with Houssem Haddar)

The mathematical modelling of electrostatic imaging methods in non-destructive testing leads to inverse boundary value problems for the Laplace equation. In principle, in these applications an unknown inclusion within a conducting host medium with constant conductivity is assessed from Cauchy data on the accessible exterior boundary of the medium. For simplicity, we assume that D_0 and D_1

are two simply connected bounded domains in $\mathbb{R}^2$ with C^2 smooth boundaries $\Gamma_0 := \partial D_0$ and $\Gamma_1 := \partial D_1$ such that $\overline{D_0} \subset D_1$ and denote by D the doubly connected domain $D := D_1 \setminus \overline{D_0}$. The determination of the unknown shape Γ_0 of a perfectly conducting inclusion D_0 is modelled by a homogeneous Dirichlet condition on Γ_0. Electrical impedance tomography for an inclusion D_0 with a constant conductivity leads to an inverse transmission problem.

For the solution of this type of inverse boundary value problems a new conformal mapping technique was developed over the last decade in a series of papers by Akduman, Haddar and Kress. We briefly describe the simplest case, i.e., the following Dirichlet boundary condition. Given a function $f \in H^{1/2}(\Gamma_1)$ we seek a harmonic function $u \in H^1(D)$ satisfying

$$(1) \qquad\qquad u = f \quad \text{on } \Gamma_1 \quad \text{and} \quad u = 0 \quad \text{on } \Gamma_0.$$

The inverse problem we are concerned with is: Given the Dirichlet data f on Γ_1 (with $f \neq 0$) and the Neumann data

$$(2) \qquad\qquad g := \frac{\partial u}{\partial \nu} \quad \text{on } \Gamma_1,$$

determine the interior boundary Γ_0. We assume the unit normal ν to Γ_1 to be directed into the exterior of D.

The main idea of the inverse method is to employ a conformal mapping between the unknown domain D and the annulus B bounded by two concentric circles C_0 with radius ρ and C_1 with radius one centered at the origin. By the conformal mapping theorem for doubly connected domains there exists a uniquely determined radius ρ and a holomorphic function Ψ that maps B bijectively onto D such that the boundaries C_0 and C_1 are mapped onto Γ_0 and Γ_1, respectively. The function Ψ is unique up to a rotation of the annulus B. In the sequel we will identify $\mathbb{R}^2$ and $\mathbb{C}$.

We parameterize the exterior boundary $\Gamma_0 = \{\gamma(t) : t \in [0, 2\pi)\}$ by a twice continuously differentiable 2π periodic function $\gamma : \mathbb{R} \to \mathbb{C}$ with the property that $\gamma|_{[0,2\pi)}$ is injective. The freedom in rotating B we fix by prescribing $\Psi(1) = \gamma(0)$ and define a boundary correspondence function $\varphi : [0, 2\pi] \to [0, 2\pi]$ by setting

$$(3) \qquad\qquad \varphi(t) := \gamma^{-1}(\Psi(e^{it})), \quad t \in [0, 2\pi].$$

The boundary values φ uniquely determine Ψ as the solution to the Cauchy problem with $\Psi|_{C_1}$ given by $\Psi(e^{it}) = \gamma(\varphi(t))$. Hence, the linear operator $N_\rho : \varphi \mapsto \chi$ where $\chi(t) := \Psi(\rho e^{it})$ for $t \in [0, 2\pi]$ is well defined. The function $\chi : [0, 2\pi] \to \mathbb{C}$ parameterizes the interior boundary curve Γ_0 and therefore determining χ solves the inverse problem. The ill-posedness of the inverse boundary value problem is reflected by the ill-posedness of the Cauchy problem, i.e., the operator N_ρ requires stabilization, for example, by Tikhonov regularization.

We now proceed with describing a nonlinear and nonlocal ordinary differential equation for the boundary correspondence function φ. To this end, we denote by $A_\rho : H^{1/2}[0, 2\pi] \to H^{-1/2}[0, 2\pi]$ the Dirichlet-to-Neumann operator for the

annulus B that maps the function F onto the normal derivative

$$(A_\rho(F))\,(t) := \frac{\partial v}{\partial \nu}\,(e^{it}), \quad t \in [0, 2\pi],$$

of the harmonic function $v \in H^1(B)$ with boundary values on C_1 and C_0 given by

$$v(e^{it}) = F(t) \quad \text{and} \quad v(\rho e^{it}) = 0 \quad \text{for} \quad t \in [0, 2\pi].$$

Via $v := u \circ \Psi$ we associate the harmonic function u in D with a harmonic function v in B. Then, from the Cauchy–Riemann equations for u and v and its conjugate harmonics the differential equation

$$(4) \qquad\qquad \varphi' = \frac{A_\rho(f \circ \gamma \circ \varphi)}{|\gamma' \circ \varphi|\, g \circ \gamma \circ \varphi}$$

for the boundary correspondence function φ can be concluded as the central piece of the inverse algorithm. The differential equation must be complemented by the boundary conditions $\varphi(0) = 0$ and $\varphi(2\pi) = \pi$. Applying Green's second integral theorem to v and $x \mapsto \ln|x|$ leads to the equation

$$(5) \qquad\qquad \rho = \exp\left(-\frac{\displaystyle\int_0^{2\pi} f(\gamma(\varphi(t)))\,dt}{\displaystyle\int_{\Gamma_1} g\,ds}\right)$$

for the radius ρ. Akduman and Kress [1] and Haddar and Kress [2] have established that the two nonlinear equations (4) and (5) (and modifications thereof) can be solved by successive iterations.

   The main advantage of this inverse algorithm is that it completely decouples the nonlinearity and the ill-posedness of the inverse boundary value problem. In the first step the boundary correspondence map φ and the radius ρ are determined iteratively from the well-posed nonlinear equations (4) and (5). Then in the second step the linear ill-posed Cauchy problem for determining Ψ from its boundary trace $\Psi|_{C_1}$ has to be solved (in the annulus B with known radius ρ). In particular, this makes the method very fast. Unfortunately, the decoupling property is lost for the extension of the method to a Robin type boundary condition and to the inverse transmission problem [3, 4, 6].

   The decoupling property is also lost for a very recent application of the above method in inverse scattering, i.e., for corresponding inverse boundary value problems for the Helmholtz equation. In addition to the Dirichlet problem (1) for the Laplace equation we consider the Dirichlet problem for a solution $u_k \in H^1(D)$ of the Helmholtz equation $\Delta u_k + k^2 u_k = 0$ with positive wave number $k > 0$ satisfying

$$(6) \qquad\qquad u_k = f \quad \text{on } \Gamma_1 \quad \text{and} \quad u_k = 0 \quad \text{on } \Gamma_0$$

and the corresponding inverse problem to recover Γ_0 from f and the Neumann data

$$(7) \qquad\qquad g_k := \frac{\partial u_k}{\partial \nu} \quad \text{on } \Gamma_1.$$

Denote the nonlinear operators that map the interior boundary Γ_0 onto the normal derivative of the solution to (1) and (6) by B and B_k, respectively. Then clearly we have that

$$(8) \qquad\qquad g = g_k + B(\Gamma_0) - B_k(\Gamma_0).$$

The above inverse algorithm for the Laplace equation defines a solution operator S that maps the Neumann data for the Laplace case to the interior boundary curve Γ_0. This operator is composed by the solution operator R for the two equations (4) and (5) that maps g onto the pair (φ, ρ) and the solution operator N_ρ for the Cauchy problem via $S = N_\rho \circ R$. Inserting this operator into (8) we obtain the fixed point equation

$$(9) \qquad\qquad g = g_k + B(S(g)) - B_k(S(g))$$

which can be used to iteratively compute the Neumann data g for the Laplace equation from the given Neumann data g_k for the Helmholtz equation. The latter then allows to retrieve $\Gamma_0 = S(g)$, or in practice approximations $\Gamma_0 \approx S(g^n)$ within the successive approximation sequence

$$(10) \qquad g^{n+1} = g_k + B(S(g^n)) - B_k(S(g^n)), \quad n = 0, 1, 2, \ldots,$$

starting with $g^0 = g_k$. Convergence has been shown for small wave numbers k provided the operator N_ρ occurring in S is regularized. Numerical examples exhibit reasonably fast convergence.

It is an open problem to extend the convergence analysis to the modification of (10) where S is replaced by $S_n := N_{\rho, \alpha_n} \circ R$ with a Tikhonov regularization N_{ρ, α_n} of the Cauchy operator N_ρ with a null sequence of regularization parameters α_n.

REFERENCES

[1] I. Akduman and R. Kress, *Electrostatic imaging via conformal mapping*, Inverse Problems **18** (2002), 1659–1672.
[2] H. Haddar and R. Kress, *Conformal mappings and inverse boundary value problems*, Inverse Problems **21** (2005), 935–953.
[3] H. Haddar and R. Kress, *Conformal mapping and an inverse impedance boundary value problem*, Jour. on Inverse and Ill-Posed Problems **14** (2006), 785–804.
[4] H. Haddar and R. Kress, *Conformal mapping and impedance tomography*, Inverse Problems **26** (2010), 074002.
[5] R. Kress, *Inverse Dirichlet problem and conformal mapping*, Mathematics and Computers in Simulation **66** (2004), 255–265.
[6] R. Kress, *Inverse problems and conformal mapping*, Complex Variables and Elliptic Equations **57** (2012), 301–316.

The factorization method for reconstructing a penetrable obstacle with unknown buried objects

Bo Zhang

(joint work with J. Yang, H. Zhang)

This talk considers the problem of scattering of time-harmonic acoustic plane waves by an inhomogeneous penetrable obstacle with buried objects inside. This type of problems occurs in various areas of applications such as radar, remote sensing, geophysics, and nondestructive testing. Let D_0 denote an impenetrable obstacle which is embedded in a penetrable obstacle D, that is, $\overline{D_0} \subset D$. Assume that $D_1 := D \setminus \overline{D_0}$ is filled with an inhomogeneous material characterized by the refractive index $n \in L^\infty(D_1)$ with $\mathrm{Re}[n(x)] > 0$ and $\Im[n(x)] \geq 0$ for almost all $x \in D_1$ and $D_2 := \mathbb{R}^3 \setminus \overline{D}$ is filled with a homogeneous material with the constant refractive index 1. Then the scattering of time-harmonic acoustic waves by D and D_0 can be modeled by the Helmholtz equation with boundary conditions on the interface ∂D and boundary ∂D_0:

$$(1) \qquad \Delta u + k^2 u = 0 \qquad \text{in } \mathbb{R}^3 \setminus \overline{D}$$

$$(2) \qquad \Delta v + k^2 n v = 0 \qquad \text{in } D \setminus \overline{D_0}$$

$$(3) \qquad u^s - v = f_1, \ \ \frac{\partial u^s}{\partial \nu} - \lambda \frac{\partial v}{\partial \nu} = f_2 \qquad \text{on } \partial D$$

$$(4) \qquad \mathscr{B}v = 0 \qquad \text{on } \partial D_0$$

$$(5) \qquad \lim_{r \to \infty} r \left(\frac{\partial u^s}{\partial r} - i k u^s \right) = 0 \qquad r = |x|,$$

where ν is the unit outward normal to the interface ∂D and boundary ∂D_0, λ is a positive constant. Here, the total field $u = u^s + u^i$ is given as the sum of the unknown scattered wave u^s which is required to satisfy the Sommerfeld radiation condition (5) and the incident plane wave $u^i = e^{ikx \cdot d}$, where d is the incident direction and k is the positive wave number given by $k = \omega/c$ in terms of the frequency ω and the sound speed c in the region D_2. On the interface ∂D, the so-called "transmission condition" (3) is imposed, which represents the continuity of the medium and equilibrium of the forces acting on it, where the boundary data $f_1 = -u^i$, $f_2 = -\partial u^i / \partial \nu$. The boundary condition $\mathscr{B}(v) = 0$ on ∂D_0 represents a Dirichlet, Neumann, impedance or mixed-type boundary condition depending on the physical property of the obstacle D_0. For simplicity we only consider the three-dimensional case and the case when D_0 is an open bounded region with a C^2 boundary ∂D_0. However, our analysis extends to the two-dimensional case and the case when D_0 is an inhomogeneous penetrable obstacle, a crack or a union of cracks and obstacles.

By the variational method it can be easily shown that the scattering problem (1)-(5) has a unique weak solution $(u, v) \in H^1_{loc}(D_2) \times H^1(D_1)$ (see, e.g. [1] for the case when n is a constant). In addition, the Sommerfeld radiation condition

(5) implies an asymptotic behavior for the scattered field u^s of the form

$$(6) \qquad u^s(x; d) = \frac{e^{ik|x|}}{|x|} \left\{ u^\infty(\widehat{x}; d) + O\Big(\frac{1}{|x|}\Big) \right\}, \qquad |x| \longrightarrow \infty$$

uniformly with respect to all directions $\widehat{x} = x/|x|$. The function u^∞ is known as the *far field pattern* of the scattered field u^s and is an analytic function of $\widehat{x}$ on the unit sphere Ω. The *inverse scattering problem* that we are concerned with is to determine the shape and location of both the penetrable obstacle D and the buried impenetrable obstacle D_0 from a knowledge of the far field pattern u^∞ for incident plane waves. The uniqueness result has been established for this inverse problem in [2] for the case when n is a known constant and in [3, 4, 5] for the case when $D_0 = \emptyset$.

Many reconstruction algorithms have been developed for solving the above inverse problem in the case when $D_0 = \emptyset$ (see, e.g., the iteration methods in [6, 7] and the singular sources method in [8] for the case when n is a known constant, the linear sampling method in [9] and the factorization method in [10, 11] for the case when $\lambda = 1$). Recently, for the case when $D_0 \neq \emptyset$, Cakoni et al. [12] introduced a multistep reciprocity gap functional method for reconstructing the interface ∂D and the buried obstacle D_0 from near field data, whilst in [13] we proposed a Newton iteration method to simultaneously reconstruct the interface ∂D and the buried obstacle D_0 from far field data.

In this talk we will prove that the factorization method can be applied to reconstruct the interface ∂D with unknown buried objects. We are motivated by [14], where the factorization method is applied to recover a penetrable obstacle without buried objects inside in inverse elastic transmission scattering. The factorization method was first suggested by Kirsch [15] for inverse obstacle scattering problems and has been extended and improved continuously since then (see the monograph [16]). Precisely, defining the far field operator $F : L^2(\Omega) \mapsto L^2(\Omega)$ by

$$(Fg)(\widehat{x}) = \int_\Omega u^\infty(\widehat{x}; d) g(d) ds(d), \qquad \widehat{x} \in \Omega,$$

we will prove the following characterization of the penetrable obstacle D (see [17]).

Theorem 1. *Assume that $\lambda > 0$ ($\lambda \neq 1$) or $\lambda = 1/n$ with $n \equiv n_0$ (some constant with $\Im(n_0) > 0$ satisfying that $\Re(n_0) > |n_0|^2$ or that $1 < \Re(n_0) < |n_0|^2$).*

For $z \in \mathbb{R}^3$ define $\phi_z \in L^2(\Omega)$ by $\phi_z(\widehat{x}) = e^{-ik\widehat{x}\cdot z}$, $\widehat{x} \in \Omega$.
Then $z \in D$ if and only if $\phi_z \in \mathcal{R}(G)$. Further, $z \in D$ if and only if

$$\sum_{j=1}^\infty \frac{|(\phi_z, \psi_j)_{L^2(\Omega)}|^2}{\lambda_j} < \infty,$$

or equivalently,

$$W(z) := \left(\sum_{j=1}^\infty \frac{|(\phi_z, \psi_j)_{L^2(\Omega)}|^2}{\lambda_j} \right)^{-1} > 0,$$

where $\{\lambda_j, \psi_j\}_{j \in \mathbb{N}}$ is an eigen-system of $F_\# := |\mathrm{Re}(F)| + \Im(F)$.

In Theorem 1 we have to assume that k is not an eigenvalue of the interior transmission problem: find $u \in H^1(D), v \in H^1(D \setminus \overline{D_0})$ such that $\Delta u + k^2 u = 0$ in D, $\Delta v + k^2 n v = 0$ in $D \setminus \overline{D_0}$, $u = v$, $\partial u / \partial \nu = \lambda \partial v / \partial \nu$ on ∂D, $\mathscr{B} v = 0$ on ∂D_0.

Note that if λ, n and $\mathscr{B}$ satisfy one of the three conditions: (1) $\lambda > 0$, $n > 0$ a.e. in $D \setminus \overline{D_0}$ and $\partial v / \partial \nu + i \rho v = 0$ on part of ∂D_0, (2) $\lambda > 0$, $\Im(n) > 0$ a.e. in $\widetilde{D} \subset D \setminus \overline{D_0}$ with $\widetilde{D} \neq \emptyset$, and $\mathscr{B} v = 0$, and (3) $\lambda = 1/n$ with $n \equiv n_1$ (a constant with $\Im(n_1) > 0$) and $\mathscr{B} v = 0$, then there are no transmission eigenvalues.

Numerical examples are provided to illustrate the inversion algorithm.

We remark that our method does not work for the case when $\mathrm{Re}(\lambda) = 1$.

References

[1] X. Liu, B. Zhang and G. Hu, *Uniqueness in the inverse scattering problem in a piecewise homogeneous medium*, Inverse Problems **26** (2010) 015002 (14pp).

[2] X. Liu and B. Zhang, *Direct and inverse obstacle scattering problems in a piecewise homogeneous medium*, SIAM J. Appl. Math. **70** (2010), 3105-3120.

[3] V. Isakov, *On uniqueness in the inverse transmission scattering problem*, Commun. Partial Diff. Equat. **15** (1990), 1565-1587.

[4] A. Kirsch and R. Kress, *Uniqueness in inverse obstacle scattering*, Inverse Prolems **9** (1993), 285-299.

[5] A. Kirsch and L. Pärvärinta, *On recovering obstacles inside inhomogeneities*, Math. Methods Appl. Sci. **21** (1998), 619-651.

[6] A. Altundag and R. Kress, *On a two-dimensional inverse scattering problem for a dielectric*, Appl. Anal., 2011, 1-15, iFirst.

[7] T. Hohage and C. Schormann, *A Newton-type method for a transmission problem in inverse scattering*, Inverse Problems **14** (1998), 1207-1227.

[8] R. Potthast and I. Stratis, *The singular sources method for an inverse transmission problem*, Computing **75** (2005), 237-255.

[9] W. Muniz, *A modified linear sampling method valid for all frequencies and an application to the inverse inhomogeneous medium problem*, Proc. Appl. Math. Mech. **5** (2005), 689-690.

[10] A. Kirsch, *Factorization of the far field operator for the inhomogeneous medium case and an application in inverse scattering theory*, Inverse Problems **15** (1999), 413-429.

[11] A. Kirsch, *The MUSIC-algorithm and the factorization method in inverse scattering theory for inhomogeneous media*, Inverse Problems **18** (2002), 1025-1040.

[12] F. Cakoni, M. Di Cristo and J. Sun, *A multistep reciprocity gap functional method for the inverse problem in a multi-layered medium*, Complex Variables and Elliptic Equations **57** (2012), 261-276.

[13] H. Zhang and B. Zhang, *A Newton type method for simultaneous reconstruction of a penetrable interface and a buried impenetrable obstacle in inverse scattering*, in preparation.

[14] A. Charalambopoulus, A. Kirsch, K.A. Anagnostopoulus, D. Gintides and K. Kiriaki, *The factorization method in inverse elastic scattering from penetrable bodies*, Inverse Problems **23** (2007), 27-51.

[15] A. Kirsch, *Characterization of the shape of a scattering obstacle using the spectral data of the far field operator*, Inverse Problems **14** (1998), 1489-1512.

[16] A. Kirsch and N. Grinberg, *The Factorization Methods for Inverse Problems*, Oxford Univ. Press, Oxford, 2008.

[17] J. Yang, B. Zhang and H. Zhang, *The factorization method for reconstructing a penetrable obstacle with unknown buried objects*, in preparation.

Transmission Eigenvalues in Inverse Scattering Theory

Fioralba Cakoni

(joint work with David Colton and Houssem Haddar)

The interior transmission problem arises in inverse scattering theory for inhomogeneous media. It is a boundary value problem for a coupled set of equations defined on the support of the scattering object and was first introduced by Colton and Monk [7] and Kirsch [10]. Of particular interest is the eigenvalue problem associated with this boundary value problem, referred to as the transmission eigenvalue problem and, more specifically, the corresponding eigenvalues which are called transmission eigenvalues. The transmission eigenvalue problem is a nonlinear and non-selfadjoint eigenvalue problem that is not covered by the standard theory of eigenvalue problems for elliptic equations. For a long time research on the transmission eigenvalue problem mainly focussed on showing that transmission eigenvalues form at most a discrete set and we refer the reader to the survey paper [8] for the state of the art on this question up to 2007. From a practical point of view the question of discreteness was important to answer, since sampling methods for reconstructing the support of an inhomogeneous medium fail if the interrogating frequency corresponds to a transmission eigenvalue. On the other hand, due to the non-selfadjointness of the transmission eigenvalue problem, the existence of transmission eigenvalues for non-spherically stratified media remained open for more than 20 years until Sylvester and Päivärinta [11] showed the existence of at least one transmission eigenvalue provided that the contrast in the medium is large enough. The story of the existence of transmission eigenvalues was completed by Cakoni, Gintides and Haddar [5] where the existence of an infinite set of transmission eigenvalue was proven only under the assumption that the contrast in the medium does not change sign and is bounded away from zero. In addition, estimates on the first transmission eigenvalue were provided. It was then showed by Cakoni, Colton and Haddar [3] that transmission eigenvalues could be determined from the scattering data and since they provide information about material properties of the scattering object can play an important role in a variety of problems in target identification.

The transmission eigenvalue problem is related to non-scattering incident fields. Indeed, if u^i is such that $u^s = 0$ then $w := u|_D$ and $v := u^i|_D$ satisfy the following homogenous problem

$$(1) \qquad\qquad \nabla \cdot A(x)\nabla w + k^2 nw = 0 \qquad \text{in } D$$

$$(2) \qquad\qquad \Delta v + k^2 v = 0 \qquad \text{in } D$$

$$(3) \qquad\qquad w = v \qquad \text{on } \partial D$$

$$(4) \qquad\qquad \nu \cdot A(x)\nabla w = \nu \cdot \nabla v \qquad \text{on } \partial D.$$

Conversely, if (1)-(4) has a nontrivial solution w and v and v can be extended outside D as a solution to the Helmholtz equation, then if this extended v is considered as the incident field the corresponding scattered field is $u^s = 0$. As will be seen later in this paper, there are values of k for which under some assumptions

on A and n, the homogeneous problem (1)-(4) has non-trivial solutions. The homogeneous problem (1)-(4) is referred to as the *transmission eigenvalue problem*, whereas the values of k for which the transmission eigenvalue problem has non-trivial solutions are called *transmission eigenvalues*. It is known, under further assumptions on the functions A and n, (1)-(4) satisfies the Fredholm property for $w \in H^1(D)$, $v \in H^1(D)$ if $A \neq I$ and for $w \in L^2(D)$, $v \in L^2(D)$ such that $w - v \in H^2(D)$ if $A = I$. Even at a transmission eigenvalue, it is not possible in general to construct an incident wave that does not scatter. This is because, in general it is not possible to extend v outside D in such away that the extended v satisfies the Helmholtz equation in all of $\mathbb{R}^d$. Nevertheless, it is already known that solutions to the Helmholtz equation in D can be approximated by entire solutions in appropriate norms. In particular let $\mathcal{X}(D) := H^1(D)$ if $A \neq I$ and $\mathcal{X}(D) := L^2(D)$ if $A = I$. Then if v_g is a Herglotz wave function defined by

$$(5) \qquad v_g(x) := \int_\Omega g(d) e^{ikx \cdot d} \, ds(d), \qquad g \in L^2(\Omega), \ \ x \in \mathbb{R}^d, \ d = 2, 3$$

where Ω is the unit $(d-1)$-sphere $\Omega := \{x \in \mathbb{R}^d : |x| = 1\}$ and k is a transmission eigenvalue with the corresponding nontrivial solution v, w, then for a given $\epsilon > 0$, there is a v_{g_ϵ} that approximates v with discrepancy ϵ in the $\mathcal{X}(D)$-norm and the scattered field corresponding to this v_{g_ϵ} as incident field is roughly speaking ϵ-small.

There two important issues concerning the transmission eigenvalues: 1) Real transmission eigenvalues can be determined from the scattered data and 2) transmission eigenvalues carry information about material properties. Therefore, transmission eigenvalues can be used to quantify the presence of abnormalities inside homogeneous media and use this information to test the integrity of materials. Next we show that it is possible to determine the real transmission eigenvalues from the scattering data. We can define the *far field operator* $F_k : L^2(\Omega) \to L^2(\Omega)$ by

$$(6) \qquad (F_k g)(\hat{x}) := \int_\Omega u_\infty(\hat{x}, d, k) g(d) \, ds(d)$$

and consider introduce the far field equation

$$(7) \qquad (F_k g)(\hat{x}) = \Phi_\infty(\hat{x}, z)$$

where $\Phi_\infty(\hat{x}, z)$ is the far field pattern of the fundamental solution $\Phi(x, z)$ of the Helmholz equation. It is known that if k is not a transmission eigenvalue, for $z \in D$ the far field equation has an approximate solution such that the corresponding Herglotz function converges in the appropriate norm. On the other hand let k be a transmission eigenvalue, $\epsilon > 0$ and let $g_{z,\epsilon}$ be such that

$$(8) \qquad \|F_k g_{z,\epsilon} - \Phi_\infty(\cdot, z)\|^2_{L^2(\Omega)} \leq \epsilon$$

with $v_{g_{z,\epsilon}}$ the corresponding Herglotz wave function. Then, in [3] it is shown that for all $z \in D$, except for a possibly nowhere dense subset, $\|v_{g_{z,\epsilon}}\|_{\mathcal{X}(D)}$ can not be bounded as $\epsilon \to 0$. Thus, transmission eigenvalues can be computed from far field data by plotting the norm of the approximate (regularized) solution of the far

field equation against frequencies and the picks in the graph indicate transmission eigenvalues.

Nest we analyze the transmission eigenvalue problem associated with the scattering problem problem for two types of inhomogeneities. First, we discuss the interior transmission problem in the case when the inhomogeneous medium has cavities, i.e. regions in which the index of refraction is the same as the host medium. In this case we establish the Fredholm property for this problem and show that transmission eigenvalues exist and form a discrete set. We also derive Faber-Krahn type inequalities for the transmission eigenvalues (see [2], [9] and [12]).

The second problem we consider is the study of the interior transmission problem corresponding to the inverse scattering by an inhomogeneous anisotropic media in which an impenetrable obstacle with Dirichlet boundary conditions is embedded. Our main focus is to understand the associated eigenvalue problem, more specifically to prove that the transmission eigenvalues form a discrete set and show that they exist. The presence of Dirichlet obstacle brings new difficulties to already complicated situation dealing with a non-selfadjoint eigenvalue problem. We employ a variety of variational techniques under various assumptions on the index of refraction as well as the size of the Dirichlet obstacle (see[1], [4] and [6] for more details).

References

[1] AS. Bonnet-BenDhia, L. Chesnel, and H. Haddar. On the use of t-coercivity to study the interior transmission eigenvalue problem. *C. R. Acad. Sci., Ser. I*, 340, 2011.

[2] F. Cakoni, D. Colton, and H. Haddar. The interior transmission problem for regions with cavities. *SIAM J. Math. Anal.*, 42(1):145–162, 2010.

[3] F. Cakoni, D. Colton, and H. Haddar. On the determination of Dirichlet or transmission eigenvalues from far field data. *C. R. Acad. Sci. Paris*, 348:379–383, 2010.

[4] F. Cakoni, A. Cossonniere and H. Haddar. Transmission eigenvalues for inhomogeneous media containing obstacles" (submitted).

[5] F. Cakoni, D. Gintides, and H. Haddar. The existence of an infinite discrete set of transmission eigenvalues. *SIAM J. Math. Anal.*, 42:237–255, 2010.

[6] F. Cakoni and A. Kirsch. On the interior transmission eigenvalue problem. *Int. Jour. Comp. Sci. Math.*, 3:142–167, 2010.

[7] D. Colton and P. Monk. The inverse scattering problem for time-harmonic acoustic waves in a inhomogeneous medium. *Quart. Jour. Mech. Applied Math.*, 41:97–125, 1988.

[8] D. Colton, L.Päivärinta, and J. Sylvester. The interior transmission problem. *Inverse Problems and Imaging*, 1:13–28, 2007.

[9] A. Cossonniere and H. Haddar. The electromagnetic interior transmission problem for regions with cavities. *SIAM J. Math. Anal.*, 43(4):1698–1715, 2011.

[10] A. Kirsch. The denseness of the far field patterns for the transmission problem. *IMA J. Appl. Math.*, 37:213–226, 1986.

[11] L.Päivärinta and J. Sylvester. Transmission eigenvalues. *SIAM J. Math. Anal*, 40:738–753, 2008.

[12] J. Sylvester. Discreteness of transmission eigenvalues via upper triangular compact operators. *SIAM J. Math. Anal.* (to appear).

Electrical impedance imaging using nonlinear Fourier transform

Samuli Siltanen

(joint work with Kim Knudsen, Matti Lassas and Jennifer L. Mueller)

Electrical impedance tomography (EIT) is an emerging medical imaging technique. In EIT, one attaches electrodes on the skin of a patient, applies voltages on the electrodes and measures the resulting electric currents. The goal of EIT is to produce an image of the internal electric conductivity. Since different tissues have different conductivities, doctors can use EIT images for detecting breast cancer or for monitoring the heart and lung function of unconscious patients. See [3].

Mathematically, EIT can be modelled by the inverse conductivity problem of Calderón [2]. Let us describe the problem in a two-dimensional setting. Let $\Omega \subset \mathbb{R}^2$ be the unit disc and let conductivity $\sigma : \Omega \to \mathbb{R}$ satisfy $0 < M^{-1} \leq \sigma(z) \leq M$. Applying voltage f at the boundary $\partial\Omega$ leads to the elliptic PDE

$$\begin{cases} \nabla \cdot \sigma \nabla u & = & 0 \text{ in } \Omega, \\ u|_{\partial\Omega} & = & f. \end{cases}$$

Boundary measurements are modelled by the Dirichlet-to-Neumann map

$$\Lambda_\sigma : f \mapsto \sigma \frac{\partial u}{\partial \vec{n}}|_{\partial\Omega}.$$

Calderón's problem is to recover σ from the knowledge of Λ_σ. In practice we do not have available the infinite-precision measurement Λ_σ, but instead have to work with a noisy measurement Λ_σ^δ satisfying $\|\Lambda_\sigma^\delta - \Lambda_\sigma\| < \delta$ with a known $\delta > 0$.

EIT is an ill-posed inverse problem: the nonlinear forward map $F : \sigma \mapsto \Lambda_\sigma$ does not have a continuous inverse. Therefore, a nonlinear regularization strategy needs to be constructed, as shown in Figure 1. For this we must define a model space X for conductivities, a data space Y for noisy measurements, and the domain $\mathcal{D}(F) \subset X$ for the forward map. Most importantly, we need to design a family of continuous mappings $\mathcal{R}_\alpha : Y \to X$ parameterized by $0 < \alpha < \infty$ and satisfying the following conditions [4, 6]. First of all, for each fixed $\sigma \in \mathcal{D}(F)$ we should get a perfect reconstruction from infinite-precision data when α tends to zero:

(1) $$\lim_{\alpha \to 0} \|\mathcal{R}_\alpha(\Lambda_\sigma) - \sigma\|_{L^\infty(\Omega)} = 0.$$

For dealing with noisy data we need to describe a choice $\alpha = \alpha(\delta)$ of regularization parameter as function of noise level such as $\alpha(\delta) \to 0$ as $\delta \to 0$. Furthermore, $\mathcal{R}_\alpha$ should be so constructed that the worst-case reconstruction error

(2) $$\sup_{\Lambda_\sigma^\delta \in Y} \left\{ \|\mathcal{R}_{\alpha(\delta)}(\Lambda_\sigma^\delta) - \sigma\|_{L^\infty(\Omega)} \ : \ \|\Lambda_\sigma^\delta - \Lambda_\sigma\|_Y \leq \delta \right\}$$

tends to zero asymptotically as $\delta \to 0$.

The traditional approach would be to define the regularized solution as the minimizer of a Tikhonov type functional, such as $\|F(\sigma) - \Lambda_\sigma^\delta\|_Y^2 + \alpha\|\sigma\|_X^2$, and compute the reconstruction iteratively. This approach has been studied for F not too nonlinear [5]. However, for strongly nonlinear problems, such as EIT, the iteration is prone to get stuck to local minima.

It is also possible to design a tailored non-iterative regularization strategy for EIT, taking into account the specific type of nonlinearity. We show how this can be done using a nonlinear low-pass filter.

Take $X = L^\infty(\Omega)$. Let $M > 0$ and $0 < \rho < 1$ and take the domain $\mathcal{D}(F)$ to be the set of functions $\sigma : \Omega \to \mathbb{R}$ satisfying $\sigma(z) \equiv 1$ for $\rho < |z| < 1$, $\|\sigma\|_{C^2(\overline{\Omega})} \leq M$ and $\sigma(z) \geq M^{-1}$. The data space Y consists of bounded linear operators $\Lambda : H^{1/2}(\partial\Omega) \to H^{-1/2}(\partial\Omega)$ satisfying $\int_{\partial\Omega} \Lambda(f)\, ds = 0$ for every $f \in H^{1/2}(\partial\Omega)$ and $\Lambda(1) = 0$. The constants M and ρ are *a priori* knowledge about the unknown conductivity. We know from [1] that the map $F : X \supset \mathcal{D}(F) \to Y$ is one-to-one.

The regularization strategy is defined as follows. Solve the boundary integral equation $\psi^\delta(\,\cdot\,, k)|_{\partial\Omega} = e^{ikz} - \mathcal{S}_k(\Lambda_\sigma^\delta - \Lambda_1)\psi^\delta$ for all $|k| < R = R(\delta)$. Here $\mathcal{S}_k$ is the single-layer operator with the exponentially behaving Faddeev Green's function as kernel. Then evaluate the truncated nonlinear Fourier transform by

$$(3) \qquad \mathbf{t}_R^\delta(k) = \begin{cases} \int_{\partial\Omega} e^{i\bar{k}\bar{z}}(\Lambda_\sigma^\delta - \Lambda_1)\psi^\delta(\cdot, k)\, ds & \text{for } |k| < R(\delta), \\[2mm] 0 & \text{for } |k| \geq R(\delta). \end{cases}$$

The step (3) can be understood as a nonlinear low-pass filtering. Here the truncation radius is defined by $R(\delta) = -\frac{1}{10}\log\delta$, and the regularization parameter is given by $\alpha(\delta) = 1/R(\delta)$.

Next, for each reconstruction point $z \in \Omega$, solve the D-bar equation

$$\frac{\partial}{\partial\overline{k}}\mu_R^\delta(z, k) = \frac{\mathbf{t}_R^\delta(k)}{4\pi\overline{k}}e^{-i(kz+\overline{k}\overline{z})}\overline{\mu_R^\delta(z, k)}$$

with asymptotic condition $\mu_R^\delta(z, \cdot) - 1 \in L^r \cap L^\infty(\mathbb{C})$. Finally, set $\mathcal{R}_{\alpha(\delta)}(\Lambda_\sigma^\delta) := (\mu_R^\delta(z, 0))^2$.

The above regularized EIT method is based on the constructive uniqueness proof [8], which was first implemented numerically in [9]. Rigorous proof for the fact that the approach really gievs a regularization strategy is given in [7].

References

[1] K. Astala and L. Päivärinta, *Calderón's inverse conductivity problem in the plane*, Annals of Mathematics, 163 (2006), pp. 265–299.

[2] A.-P. Calderón, *On an inverse boundary value problem*, in Seminar on Numerical Analysis and its Applications to Continuum Physics (Rio de Janeiro, 1980), Soc. Brasil. Mat., Rio de Janeiro, 1980, pp. 65–73.

[3] M. Cheney, D. Isaacson, and J. C. Newell, *Electrical impedance tomography*, SIAM Review, 41 (1999), pp. 85–101.

[4] H. Engl, M. Hanke, and A. Neubauer, *Regularization of inverse problems*, Kluwer Academic Publishers, 1996.

[5] B. Kaltenbacher, A. Neubauer, and O. Scherzer, *Iterative regularization methods for nonlinear ill-posed problems*, vol. 6, de Gruyter, 2008.

[6] A. Kirsch, *An introduction to the mathematical theory of inverse problems*, Springer-Verlag, second ed., 2011.

[7] K. Knudsen, M. Lassas, J. Mueller, and S. Siltanen, *Regularized D-bar method for the inverse conductivity problem*, Inverse Problems and Imaging, 3 (2009), pp. 599–624.
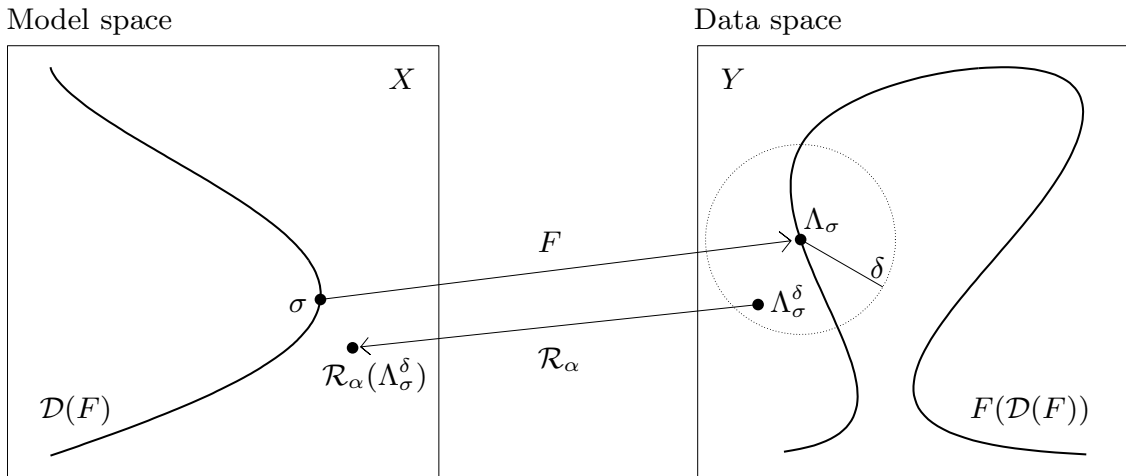
Model space

Data space

FIGURE 1. Schematic illustration of nonlinear regularization of the EIT problem. Here $\mathcal{R}_\alpha : Y \to X$ must be continuous.
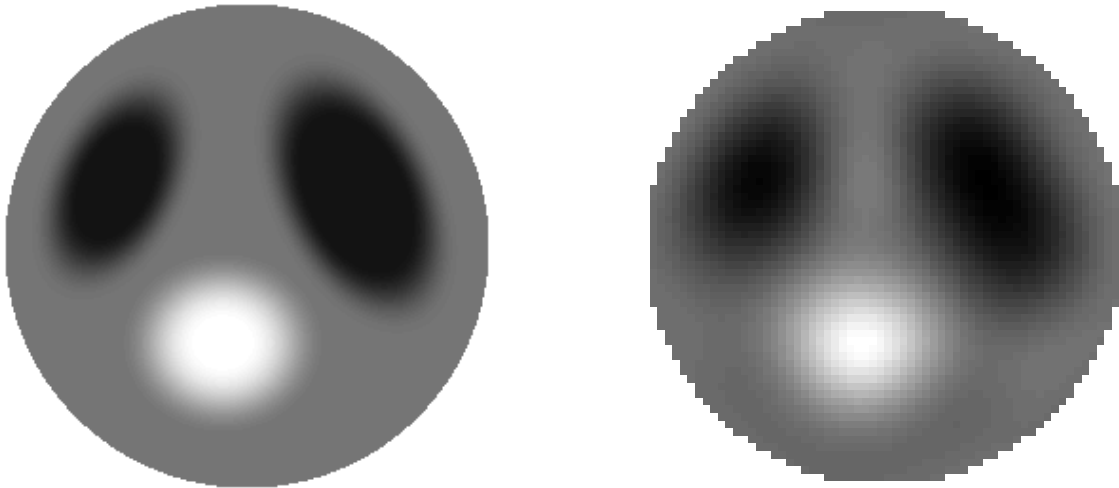

FIGURE 2. Reconstruction of a conductivity using the regularized D-bar method. Left: original conductivity. Right: reconstruction. Here $\delta = 10^{-6}$ and $R = 6.7$.

[8] A. I. NACHMAN, *Global uniqueness for a two-dimensional inverse boundary value problem*, Annals of Mathematics, 143 (1996), pp. 71–96.

[9] S. SILTANEN, J. MUELLER, AND D. ISAACSON, *An implementation of the reconstruction algorithm of A. Nachman for the 2-D inverse conductivity problem*, Inverse Problems, 16 (2000), pp. 681–699.

Reporter: Oleksandr Bondarenko